Stable oxygen isotopes and Mg/Ca in planktic foraminifera from modern surface sediments of the Western Pacific Warm Pool: Implications for thermocline reconstructions

Martina Hollstein[1*], Mahyar Mohtadi[1], Yair Rosenthal[2], Paola Moffa Sanchez[3], Delia Oppo[4], Gema Martínez Méndez[1], Stephan Steinke[5], Dierk Hebbeln[1]

[1]MARUM – Center for Marine Environmental Sciences, University of Bremen, Bremen, Germany

[2]Department of Marine and Coastal Sciences and Earth and Planetary Sciences, Rutgers, State University of New Jersey, USA.

[3]School of Earth and Ocean Sciences, Cardiff University, Cardiff, UK

[4]Department of Geology and Geophysics, Woodshole Oceanographic Institution, Massachusetts, USA

[5]Department of Geological Oceanography, Xiamen University, Xiamen, China

*Corresponding author: Martina Hollstein (mhollstein@marum.de)

Key Points:

- Combined Mg/Ca and stable oxygen isotopes in planktic foraminifera tests from accurately dated modern surface sediments
- Seawater oxygen isotope-salinity regressions for surface and subsurface waters in the Western Pacific Warm Pool
- Calcification depth estimates and regional multispecies and species-specific Mg/Ca-temperature calibrations

Abstract

Mg/Ca and stable oxygen isotope compositions ($\delta^{18}O$) of planktic foraminifera tests are commonly used as proxies to reconstruct past ocean conditions including variations in the vertical water column structure. Accurate proxy calibrations require thorough regional studies, since parameters such as calcification depth and temperature of planktic foraminifera depend on local environmental conditions. Here we present radiocarbon-dated, modern surface sediment samples and water column data (temperature, salinity, seawater $\delta^{18}O$) from the Western Pacific Warm Pool. Seawater $\delta^{18}O$ ($\delta^{18}O_{SW}$) and salinity are used to calculate individual regressions for western Pacific surface and thermocline waters ($\delta^{18}O_{SW} = 0.37*S-12.4$ and $\delta^{18}O_{SW} = 0.33*S-11.0$). We combine shell $\delta^{18}O$ and Mg/Ca with water column data to estimate calcification depths of several planktic foraminifera and establish regional Mg/Ca-temperature calibrations. *Globigerinoides ruber, Globigerinoides elongatus* and *Globigerinoides sacculifer* reflect mixed layer conditions. *Pulleniatina obliquiloculata* and *Neogloboquadrina dutertrei* and *Globorotalia tumida* preserve upper and lower thermocline conditions, respectively. Our multispecies Mg/Ca-temperature calibration (Mg/Ca = 0.26exp0.097*T) matches published regressions. Assuming the same temperature sensitivity in all species, we propose species-specific calibrations that can be used to reconstruct upper water column temperatures. The Mg/Ca-temperature dependencies of *G. ruber, G. elongatus* and *G. tumida* are similar to published equations. However, our data imply that calcification temperatures of *G. sacculifer*, *P. obliquiloculata* and *N. dutertrei* are exceptionally warm in the western tropical Pacific, and thus, underestimated by previously published calibrations. Regional Mg/Ca-temperature relations are best described by Mg/Ca = 0.24exp0.097*T for *G. sacculifer* and by Mg/Ca = 0.21exp0.097*T for *P. obliquiloculata* and *N. dutertrei*.

1. Introduction

The Western Pacific Warm Pool (WPWP) is a major source of heat and water vapor to the global atmosphere with far-reaching climate impacts [e.g. *Gagan et al.*, 2004]. The area is also thought to play an essential role in the global overturning circulation, because it provides waters to the Pacific equatorial current system and the Indonesian Throughflow, [e.g. *Gordon*, 1986]. Present climate in the WPWP is mainly controlled by the Austral-Asian monsoon system and large-scale climate phenomena such as the El Niño Southern Oscillation (ENSO). The regional climate is strongly coupled to ocean conditions. Changes in the prevailing climate conditions affect, for example, mixed layer depth and the thermocline structure [e.g. *DiNezio et al.*, 2011; *Vecchi et al.*, 2006]. Thus, reconstructing past hydrographic conditions and variations in the vertical structure of the water column allow to draw conclusions on the regional WPWP climate evolution.

There is an ongoing debate how the thermocline depth varied throughout the past. For example, some records indicate a thermocline deepening during the Last Glacial Maximum (LGM) [e.g.

Bolliet et al., 2011], others indicate a thermocline shoaling during the same period [*Andreasen and Ravelo*, 1997; *Beaufort et al.*, 2001; *de Garidel-Thoron et al.*, 2007; *Regoli et al.*, 2015; *Sagawa et al.*, 2012] and yet others indicate no change compared to the modern ocean [*Patrick and Thunell*, 1997]. Many of these reconstructions are based on the calculation of differences between shell Mg/Ca-derived temperature and/or $\delta^{18}O$ of planktic foraminifera calcifying at different depth levels to estimate vertical temperature gradients within the upper water column [e.g. *Bolliet et al.*, 2011; *de Garidel-Thoron et al.*, 2007; *Regoli et al.*, 2015]. Previous studies used for example the difference between shell Mg/Ca in *G. ruber* as surface indicator and *P. obliquiloculata* or *N. dutertrei* as thermocline depth indicators [e.g. *Bolliet et al.*, 2011], or the difference between *G. ruber* sensu stricto and *G. ruber* sensu lato (here referred to as *G. ruber* and *G. elongatus* following *Aurahs et al.* [2011]) [*Regoli et al.*, 2015]. However, to choose species and interpret such proxy records correctly, it is essential to understand how modern hydrographic conditions are reflected in foraminiferal calcite.

The choice of species to use depends on regional calcification depths, which are determined by the species preferences and local environmental conditions. However, although many paleoclimate reconstructions for the WPWP exist, precise estimates of calcification depths are sparse in this area. Published reconstructions rely on plankton tow and sediment trap studies in the central equatorial Pacific, North Pacific or Indian Ocean [*Kawahata et al.*, 2002; *Kuroyanagi and Kawahata*, 2004; *Mohtadi et al.*, 2011; *Peeters et al.*, 2002; *Rippert et al.*, 2016; *Watkins et al.*, 1996]. In addition, precise Mg/Ca-temperature calibrations are a prerequisite to convert Mg/Ca into temperature. For the WPWP there are only two regional Mg/Ca-temperature calibrations [*Lea et al.*, 2000; *Sagawa et al.*, 2012]. *Lea et al.* [2000] provide a species-specific calibration for *G. ruber* and *Sagawa et al.* [2012] present a multispecies calibration. Both calibrations are exposed to certain limitations. While the species-specific calibration might be biased by post-depositional effects on the core top planktic foraminifera sample material [*Lea et al.*, 2000], the multispecies equation of *Sagawa et al.* [2012] bases only on data from a single station. Besides, both calibrations base on late Holocene sediments and therefore, might lack comparability to present hydrography. Regional species-specific calibrations for subsurface planktic foraminifera species do not exist for the WPWP. Subsequently, most proxy studies use Mg/Ca-temperature calibrations from other areas [e.g. *Bolliet et al.*, 2011; *de Garidel-Thoron et al.*, 2007; *Regoli et al.*, 2015; *Tachikawa et*

al., 2014]. However, the adequacy of previously published Mg/Ca-temperature calibrations for the WPWP has not yet been tested.

Here, we present paired Mg/Ca and $\delta^{18}O$ measurements on planktic foraminifera tests from radiocarbon-dated, modern surface sediments in combination with water column data from stations offshore the Philippines and Papua New Guinea (PNG) (Figure 1a and Table 1). Together, these areas represent a major part of the WPWP. We estimate species-specific calcification depths and temperatures of various planktic foraminifera species and establish regional Mg/Ca temperature calibrations for the WPWP. In order to estimate calcification depths, we compare shell $\delta^{18}O$ with depth profiles of expected equilibrium $\delta^{18}O$ of calcite ($\delta^{18}O_C$) at the respective locations. While this is a common approach, an advantage of our study is the availability of concurrently measured salinity and seawater $\delta^{18}O$ ($\delta^{18}O_{SW}$) data, upon which the calculated depth profiles of $\delta^{18}O_C$ are based on. In this framework, we also calculate and provide regional $\delta^{18}O_{SW}$-salinity regressions for surface and subsurface water masses in the WPWP. Finally, we relate Mg/Ca to calcification temperatures to find the most appropriate Mg/Ca calibration for each species and establish a regional multispecies as well as monospecific Mg/Ca-temperature calibrations. We identify the appropriate species to reconstruct past variations in mixed layer depth and thermocline structure as well as the appropriate calibrations to convert Mg/Ca into temperature.

We note that the study is subject to certain limitations. First, it is based on surface sediments. This bears the disadvantages that we do not have direct information about hydrographic parameters at periods, when the calcite shells were built. Besides, we cannot fully exclude secondary influences (e.g. dissolution) on our data and, we cannot resolve (intra-)seasonal changes in hydrography. Second, our study includes water column data measured during two expeditions. These data provide only snapshots of the WPWP hydrography. Moreover, we did not measure pH or $[CO_3^{2-}]$ and therefore, cannot fully exclude an effect of pH or $[CO_3^{2-}]$ on shell Mg/Ca, although it appears negligible under ambient seawater conditions [*Kısakürek et al.*, 2008; *Russell et al.*, 2004]. Third, since the availability of modern sample material is a prerequisite for calibration studies, our sites are exclusively located in the coastal WPWP, where sedimentation rates are higher than in the open Pacific Ocean. The applicability of our calibrations for the open ocean WPWP needs to be tested in future studies. Finally, especially species-specific calibrations are restricted by the fact,

that the temperature range within the study area is rather small. Where necessary, we discuss the limitations of the data in more detail (see section 5). Overall, the strengths of this study outweigh the mentioned limitations. Sediment-based studies have the great advantage that they are performed on the same material used for paleo studies. In relation to this, a great advantage of our study is the availability of (radiocarbon) dated, modern surface sediments. In addition, as mentioned above, our study greatly benefits from concurrent measurements of temperature, salinity and $\delta^{18}O_{SW}$.

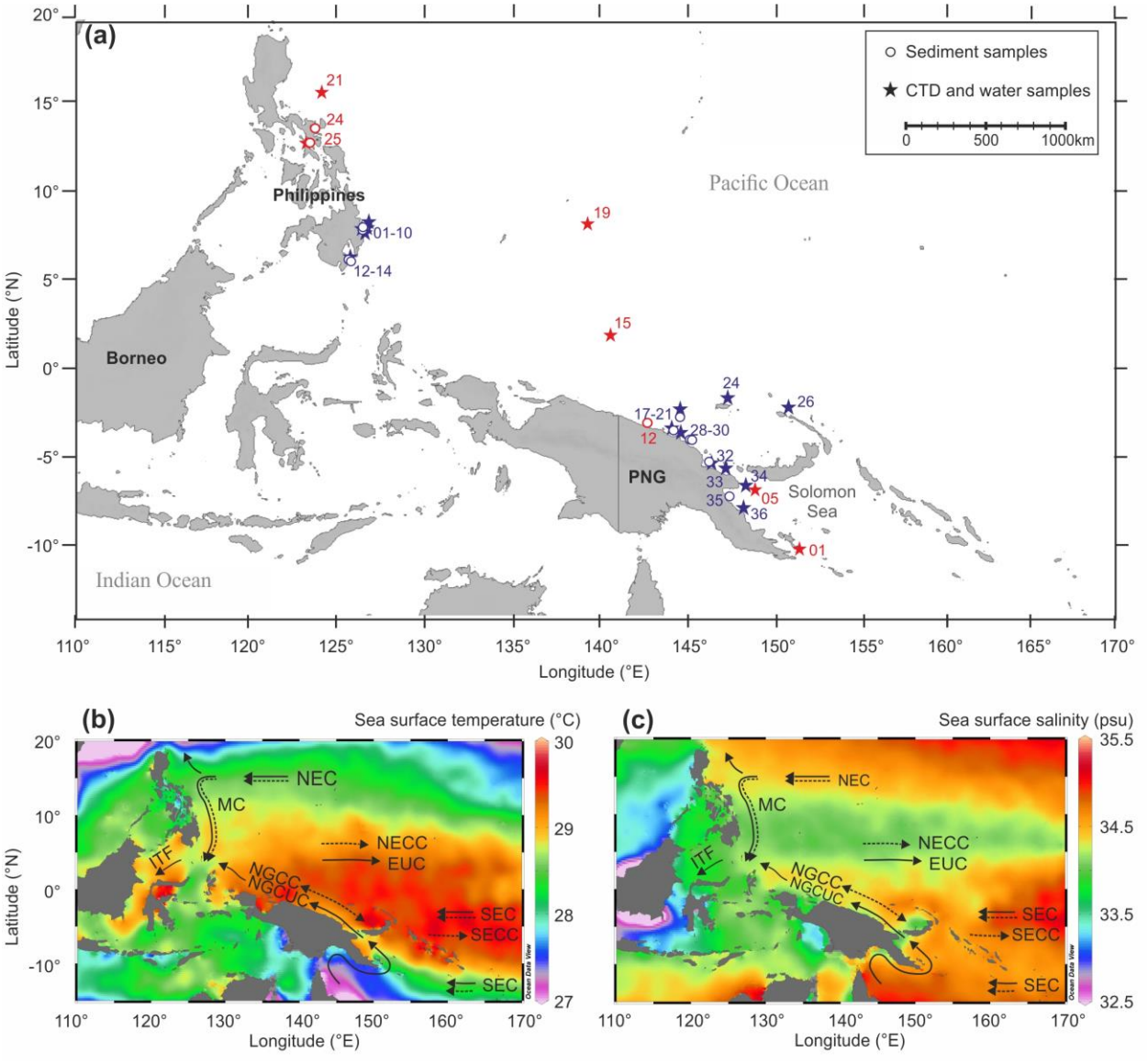

Figure 1. (a) Schematic map of the study area showing the stations, where water column data (stars) and surface sediments (dots) were collected during expeditions SO-228 (blue) and RR-1313

(red). Sites are labelled with station numbers. (b) Mean annual sea surface temperature and (c) sea surface salinity derived from WOA13 [*Locarnini et al.*, 2013; *Zweng et al.*, 2013]. Temperature and salinity maps were created with the Ocean data view software [*Schlitzer*, 2014]. Dashed and solid arrows indicate main surface and (sub)surface currents influencing the study sites. MC – Mindanao Current, NEC – North Equatorial Current, NECC – North Equatorial Counter Current, EUC – Equatorial Undercurrent, NGCC – New Guinea Coastal Current, NGCUC – New Guinea Coastal Undercurrent, SEC – South Equatorial Current, SECC – South Equatorial Countercurrent, ITF – Indonesian Throughflow.

146

147 **Table 1.** Shell stable oxygen isotopes and Mg/Ca ratios of various planktic foraminifera species in surface sediments from the

148 Western Pacific Ocean.

Core	Latitude (°N)	Longitude (°E)	Water depth (m)	*G. ruber* $\delta^{18}O$ (‰ VPDB)	*G. ruber* Mg/Ca (mmol/mol)	*G. elongatus* $\delta^{18}O$ (‰ VPDB)	*G. elongatus* Mg/Ca (mmol/mol)	*G. sacc.* $\delta^{18}O$ (‰ VPDB)	*G. sacc.* Mg/Ca (mmol/mol)	*P. obliq.* $\delta^{18}O$ (‰ VPDB)	*P. obliq.* Mg/Ca (mmol/mol)	*N. dutertrei* $\delta^{18}O$ (‰ VPDB)	*N. dutertrei* Mg/Ca (mmol/mol)	*G. tumida* (355-425 µm) $\delta^{18}O$ (‰ VPDB)	*G. tumida* (355-425 µm) Mg/Ca (mmol/mol)	*G. tumida* (>425 µm) $\delta^{18}O$ (‰ VPDB)	*G. tumida* (>425 µm) Mg/Ca (mmol/mol)
Philippines																	
RR1313-24 50MC	13.57	123.73	1055	-3.25 -3.15	5.28	-3.24	-	-2.78	3.81	-3.47	3.17	-1.84	-	-	-	-	-
RR1313-25 53MC	12.78	123.48	559	-2.95	5.30	-3.30	-	-	3.95	-	-	-	4.23	-	-	-	-
GeoB 17404-2	7.90	126.54	404	-3.03	5.47	-2.91	-	-2.69	3.95	-	-	-	-	-	-	-	-
GeoB 17410-3	7.87	126.59	771	-3.08	5.44 5.82	-3.79	5.46	-3.16 -2.89 -2.94 -2.55 -2.47	4.04	-	-	-	2.68	-	3.27	-	-
GeoB 17414-2	6.26	125.83	2188	-3.13	4.95	-3.01	-	-2.90	3.55	-2.34	2.69 2.74	-2.31 -2.23 -2.23 -2.12 -2.07	2.62	-	-	-	-
Papua New Guinea																	
GeoB 17419-2	-2.81	144.50	1887	-3.18 -3.14 -3.10 -3.15 -2.90	5.17 5.30	-3.05	5.37	-2.95	3.77	-2.15 -1.80 -1.69 -1.59 -1.57	2.27 2.51	-1.64	2.30	-0.70 -0.64 -0.16	1.79 1.89	-0.94	1.63
RR1313-12 30MC	-3.13	142.76	994	-3.74	5.30	-3.01	-	-3.39	4.26	-2.40	2.91	-	2.59	-	-	-	-
GeoB 17421-2	-3.55	144.20	588	-3.45	4.94	-3.43	5.42	-2.64	3.66	-2.20	2.70	-1.52 -1.42 -1.35 -1.27	1.95	-0.31	2.15	-	-
GeoB 17429-1	-4.10	145.20	1604	-3.02	5.13	-3.04 -2.81 -2.77 -2.73 -2.59	5.21	-2.62	3.74 3.85	-2.00	2.93	-2.01	2.24 2.39	-0.07	1.41	-0.08	1.72
GeoB 17430-2	-4.22	145.03	1160	-3.38 -3.31 -3.02 -2.98 -2.78	5.19	-2.98	5.14	-2.73	3.89 4.03	-2.15	2.80	-1.75	2.78	-0.01	1.43 1.76	-0.31	1.90
GeoB 17432-3	-5.34	146.20	1388	-3.24	5.30	-2.86	5.14 5.44	-2.62 -2.60 -2.60 -2.47 -1.72	3.58	-2.13	2.63	-2.09	1.54 3.09	-	1.35	0.06	1.56
GeoB 17435-2	-7.27	147.34	1001	-3.29	5.10 5.77	-3.24 -3.02 -2.89 -2.24	5.68	-2.81	3.88	-2.23	2.70 2.71	-2.09	2.26	-0.15	1.68	-0.45 -0.35 -0.08	1.43 1.85

2. Study area

The WPWP is characterized by exceptionally high ocean temperatures with sea surface temperatures (SST) exceeding 28°C (Figure 1b) [*Locarnini et al.*, 2013]. Sea surface salinity is about 34 psu (Figure 1c) [*Zweng et al.*, 2013]. The average mixed layer depth is about 50–100 m [*Locarnini et al.*, 2013]. The upper thermocline waters are characterized by higher salinities with maxima of around 34.5–35.0 psu off the Philippines and 35.5 psu off PNG. Salinity maxima correspond to the North and South Pacific Tropical Waters (NPTW and SPTW). The NPTW is formed within the western North Pacific Subtropical Gyre and transported along the Philippines towards the equator by the Mindanao Current (MC) [*Fine et al.*, 1994]. The SPTW originates in the South Pacific Suptropical Gyre [*Tsuchiya et al.*, 1989]. It is transported westwards by the SEC and along the coast of PNG by the New Guinea Coastal Current (NGCC) and Undercurrent (NGCUC) system. Below the NPTW and SPTW waters are characterized by lower salinities and are influenced by the Antarctic Intermediate Water (AAIW) originating in the Southern Ocean and/or the North Pacific Intermediate water (NPIW) with stronger predominance of AAIW offshore PNG and of NPIW offshore the Philippines [*Fine et al.*, 1994; *Zenk et al.*, 2005].

The seasonal climate variability is mainly controlled by the Austral-Asian monsoon and leads to only minor changes in the WPWP hydrography. Temperature and salinity variations are smaller than 1-2°C and 1 psu [*Locarnini et al.*, 2013; *Zweng et al.*, 2013]. On interannual timescales, El Niño Southern Oscillation (ENSO) affects surface ocean conditions as well as the vertical structure of the water column in the WPWP with drier (wetter) conditions and a shallower (deeper) thermocline during El Niño (La Niña) years.

Generally, the northern part of the study area is characterized by oligotrophic surface conditions and a deep chlorophyll maximum (DCM) at the top of the thermocline [*Radenac and Rodier*, 1996]. North of PNG nutrient concentrations and biological productivity are higher than elsewhere in the WPWP [*Radenac et al.*, 2016]. However, the (vertical) distribution of nutrients and chlorophyll is variable on (intra-)seasonal timescales [e.g. *Higgins et al.*, 2006; *Radenac and Rodier*, 1996; *Radenac et al.*, 2016].

The (intra-)seasonal distribution of planktic foraminifera is controlled by different factors, such as temperature, salinity and the availability of light and nutrients. Sediment trap data do not

reveal a clear picture of (intra-)seasonal preferences of planktic foraminifera in the study area [*Kawahata et al.*, 2002; *Yamasaki et al.*, 2008]. Flux data from the equatorial Pacific showed large (small) peaks during boreal summer (winter) under El Niño conditions and an increased shell flux during the first half of the year under La Niña conditions [*Kawahata et al.*, 2002; *Yamasaki et al.*, 2008]. Since no clear (intra-)seasonal pattern is indicated by these data we assume that planktic foraminifera calcify perennially in the WPWP.

3. Materials and methods

3.1. Water column data and $\delta^{18}O_{SW}$–salinity regressions

For this study, we used profiles of water column data, measured at fifteen stations offshore the Philippines and PNG in May-June 2013 during RV SONNE expedition SO-228 [*Mohtadi et al.*, 2013] and at six stations in August 2013 during RV REVELLE expedition RR-1313 (Figure 2) [*Rosenthal,* unpublished]. Temperature and salinity profiles are based on CTD (Conductivity, Temperature and Depth) data. CTD data were measured using Seabird SBE911 (plus) CTD profilers during both expeditions. During CTD casts, water samples for stable isotope analyses were collected from several water depths (supplementary information, Table S1). Sampling was performed with CTD-sampling rosettes equipped with 24 Niskin bottles of 10–15 l volume. A part of the collected water was siphoned into 100 ml glass bottles for stable isotope analyses, care was taken to avoid getting bubbles in the samples [*Mohtadi et al*., 2013; *Rosenthal,* unpublished]. All SO-228 samples (labelled as GeoB-samples in Table 1) were sealed with wax and stored at 4°C before analysis. $\delta^{18}O_{SW}$ was determined with a Picarro L1102-i CRDS water analyser with vaporization module V1102-i coupled to a CTC/Leaptec PAL auto sampler at the Department of Geography and Earth Sciences, University of Erlangen-Nuremberg. Calibration against Vienna Standard Mean Ocean Water (VSMOW) was achieved by calibration to laboratory water standards calibrated against IAEA-standards VSMOW2 and SLAP2 [*van Geldern and Barth*, 2012]. External reproducibility was 0.05 ‰. For the RR1313 samples, δ^{18}Osw measurements were made at Rutgers University, New Jersey on a FISONS OPTIMA Mass Spectrometer equipped with a MicroMass Multiprep automatic sample processing system after water sample equilibration with CO_2 using standard methods [*Epstein and Mayeda*, 1953; *Fairbanks*, 1982]. All samples were run in duplicate. Precision was estimated to be ±0.03 ‰ (1 σ) as determined by multiple (n = 12) daily analyses of a laboratory standard. Replicates must measure to within 0.068 ‰ to be included in the final data set.

Instrument linearity and accuracy was determined by comparison of the laboratory standard to NBS standard water VSMOW, GISP, and SLAP. Accuracy was estimated to be within 0.03 ‰ by comparison of measurements of North Atlantic Bottom Water with VSMOW.

Generally, $\delta^{18}O_{SW}$ is linearly related to salinity [*Craig and Gordon*, 1965; *Fairbanks et al.*, 1992]. However, since both parameters are controlled by a number of factors, intercept and slope of their relation are not the same for all ocean regions. Therefore, regional calibrations are required [*LeGrande and Schmidt*, 2006]. Because the $\delta^{18}O_{SW}$–salinity relation is not constant over depth, we generated separate equations for surface and subsurface (SPTW and NPTW) waters. For both, we investigated individual relations for the areas offshore the Philippines and PNG as well as combined, more general, relations representing the entire study area. We do not necessarily consider water samples from all stations and depth intervals. Rather, for each equation we include samples that best characterize the relevant water masses (supplementary information, Figure S1). The SPTW and NPTW regressions include only samples that represent the core of these water masses, the WPWP wide subsurface regression is more general and covers a slightly wider depth range.

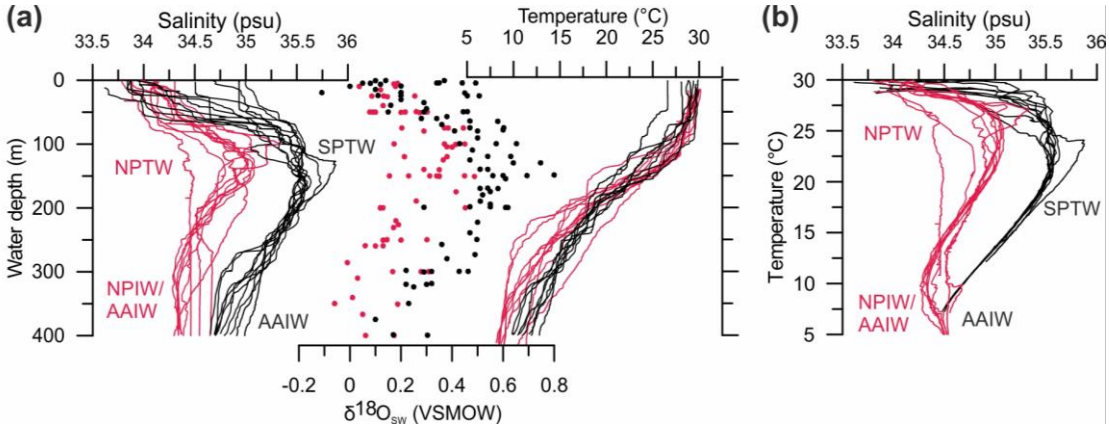

Figure 2. (a) Salinity, $\delta^{18}O_{SW}$ and temperature profiles and (b) Temperature-salinity relations at stations offshore the Philippines (red) and Papua New Guinea (black). Water masses are labeled as follows: NPTW – North Pacific Tropical Water, SPTW – South Pacific Tropical Water, NPIW – North Pacific Intermediate Water, AAIW – Antarctic Intermediate Water.

3.2. Sediment samples

Surface sediments were collected with multicorer devices during expedition SO-228 (nine sampling sites) [*Mohtadi et al.*, 2013] and during expedition RR-1313 (three sampling sites)

[*Rosenthal et al.*, unpublished]. The upper one or two cm of each multicore were washed over 63 µm sieves and dried.

All core sites are situated well above the present lysocline depth of 3300 m where carbonate preservation is expected to be good [see *Berger et al.*, 1982 and references therein]. Presence of aragonitic pteropod shells in most SO-228/GeoB core tops (including the core top from our deepest site) further indicate a good carbonate preservation in our samples.

3.3. Dating

Age estimates of all GeoB sediment samples are based on accelerator mass spectrometry (AMS) ^{14}C ages (Table 2). All ^{14}C ages were measured on monospecific *Globigerinoides sacculifer* or on mixed *Globigerinoides ruber, G. elongatus* and *G. sacculifer* samples. The measurements were carried out at the Keck Carbon Cycle Accelerator Mass Spectrometry Laboratory, University of California, Irvine (UCI). Fraction modern carbon ($F^{14}C$) values above one indicate modern ages for all ^{14}C dated samples (Table 2). In addition, a few GeoB samples were treated with Rose Bengal and contained stained individuals, indicating that these individuals died only very recently.

The RR-1313 samples did not contain enough foraminifera for radiocarbon dating. For age control of these samples, we measured the carbon isotopic composition ($\delta^{13}C$) on about 10 specimens of *G. ruber* from the 250-300 µm size fraction from the upper 10 cm of each multicore to check for the Suess effect (Figure S2). The Suess effect describes a rapid decrease in seawater $\delta^{13}C$ going along with the depletion in ^{13}C of atmospheric CO_2, which has been caused by an increase in deforestation and burning of ^{12}C rich fossil fuels since the industrial revolution [e.g. *Böhm et al.*, 1996; *Friedli et al.*, 1986]. The $\delta^{13}C$ measurements were performed at Rutgers University, New Jersey using a Micromass Optima mass spectrometer, coupled to an automatic line for carbonate preparation. The stable isotope values were calibrated against the international Vienna Pee Dee Belemnite (VPDB) standard using an internal standard, which is calibrated against the National Bureau of Standards (NBS) 19 standard. The long-term standard deviation for $\delta^{13}C$ was 0.06 ‰. Rapid drops in $\delta^{13}C$ from our RR-1313 multicores are indicative for Suess effect and hence, modern ages of these surface sediments (Figure S2). Thus, all samples used in this study reflect modern hydrographic conditions of the WPWP.

Table 2. Radiocarbon dating of surface sediments from the Western Pacific Warm Pool. Results are expressed as fraction modern carbon ($F^{14}C$) and conventional ^{14}C ages.

Core	Lab-ID	Depth (cm)	Species	$F^{14}C$ ± error	^{14}C age ± error (years)	Cal. Age
GeoB 17404-2	142715	1-2	*G. ruber, G. elongatus, G. sacculifer*	1.042 ± 0.002	-325 ± 20	>1950 AD
GeoB 17410-3	158806	1-2	*G. ruber, G. elongatus, G. sacculifer*	1.064 ± 0.002	-490 ± 20	>1950 AD
GeoB 17414-2	158804	0-1	*G. ruber, G. elongatus, G. sacculifer*	1.058 ± 0.002	-445 ± 20	>1950 AD
GeoB 17419-2	142718	0-1	*G. sacculifer*	1.072 ± 0.002	-550 ± 20	>1950 AD
	142719	0-1	*G. sacculifer*	1.068 ± 0.003	-515 ± 20	>1950 AD
GeoB 17421-2	158805	0-1	*G. ruber, G. elongatus, G. sacculifer*	1.054 ± 0.002	-420 ± 15	>1950 AD
GeoB 17429-1	142725	0-1	*G. sacculifer*	1.054 ± 0.002	-415 ± 20	>1950 AD
GeoB 17430-2	142717	0-1	*G. ruber, G. elongatus, G. sacculifer*	1.058 ± 0.002	-445 ± 20	>1950 AD
GeoB 17432-3	142716	0-1	*G. sacculifer*	1.049 ± 0.002	-375 ± 20	>1950 AD
GeoB 17435-2	158803	0-1	*G. sacculifer*	1.066 ± 0.002	-500 ± 20	>1950 AD

3.4. Isotope and trace element analyses

Tests from the foraminiferal species *G. ruber*, *G. elongatus* and *G. sacculifer* (without sac-like final chamber) (all taken from the 250–355 µm size fraction), *Neogloboquadrina dutertrei* and *Pulleniatina obliquiloculata* (355–425 µm), and *Globorotalia tumida* (355–425 µm and >425 µm) were picked under a binocular for $\delta^{18}O$ and Mg/Ca analyses. For all species but *G. tumida*, specimens were separately picked for isotope and Mg/Ca analyses. *G. tumida* specimens were very rare in most of the samples. In order to ensure that fragments of several individuals were used for each measurement, 10 (where available) individuals were picked, crushed, homogenized and then separated for isotope and trace element analyses.

Around 40-120 µg carbonate (around 3–10 specimens) were used for stable isotope analyses. The isotopic composition of all samples was measured at the MARUM-isotope laboratory, University of Bremen, Germany, using a Finnigan MAT 251 mass spectrometer, connected to an automatic line for carbonate preparation (type "Kiel III"). All isotope values were calibrated against the international Vienna Pee Dee Belemnite (VPDB) standard. The internal carbonate standard is a Solnhofen Limestone, which is calibrated to the NBS 19 standard. The analytical

293 standard deviation for $\delta^{18}O$ is below ±0.07 ‰. To check the reproducibility of the data we
294 performed up to four (depending on the available material) replicate measurements on 11
295 samples (Table 1). The results indicate an average standard deviation of 0.22 ‰ for $\delta^{18}O$.
296
297 For Mg/Ca analyses we used 30 (where available) well preserved specimens of *G. ruber* and
298 *G. elongatus*, 25 specimens of *G. sacculifer*, 15 specimens of *P. obliquiloculata* and *N.*
299 *dutertrei* and between 2 and 10 individuals of *G. tumida*. Although the presence of pteropods
300 indicates negligible effect of carbonate dissolution, all samples were weighed to estimate a
301 potential influence of dissolution on the Mg/Ca records. Samples were gently crushed between
302 two glass plates to open the chambers. The full trace metal cleaning procedure followed the
303 protocol described by *Barker et al.* [2003] with an additional reductive step [*Boyle and*
304 *Keigwin*, 1985; *Rosenthal et al.*, 1997; *Rosenthal et al.*, 1999]. Samples were dissolved in
305 0.0065 M HNO_3, centrifuged for 10 min at 10000 rpm and diluted with 0.5 N HNO_3. The final
306 calcium concentration of the samples was on average 3.2 mM. Trace metal ratios were
307 measured at Rutgers University, New Jersey with a Thermo Fisher/Finnigan Element XR
308 sector-field inductively coupled plasma mass spectrometer (ICP-MS). Mg/Ca measurements
309 were performed in low resolution ($\Delta m/m = 300$). Measured ratios were blank corrected. Mass
310 drift and matrix effects and the long term precision of the data were controlled with in house
311 standard solutions [*Rosenthal et al.*, 1999]. All Mg/Ca values are given in mmol/mol. Replicate
312 measurements on 14 samples revealed an average standard deviation of 0.23 mmol/mol (Table
313 1). To monitor the cleaning efficacy Al/Ca, Fe/Ca and Mn/Ca were measured alongside Mg/Ca.
314 None of these ratios showed a covariance with Mg/Ca (Figure S3). Mg/Ca ratios of individual
315 species do not show a correlation to water depth or shell normalized weights (Figure S4). Thus,
316 we exclude any substantial effect of carbonate dissolution on shell Mg/Ca values.
317

318 ### 3.5. Estimation of calcification depths and temperatures

319 In order to estimate species-specific calcification depths we compare shell $\delta^{18}O$ of individual
320 species with depth-profiles of $\delta^{18}O_C$, assuming that all species calcified in isotopic equilibrium
321 with seawater. The water depth where shell $\delta^{18}O$ matches the expected $\delta^{18}O_C$ is considered to
322 reflect the calcification depth of the respective species at the site.
323 Depth-profiles of expected $\delta^{18}O_C$ were calculated from SO-228 and RR-1313 CTD salinity
324 profiles as follows. First, $\delta^{18}O_{SW}$ was calculated from salinity using here established regional
325 (WPWP) $\delta^{18}O_{SW}$-salinity equations (equations I and II in section 4.1). The average uncertainty

in the calculated $\delta^{18}O_{SW}$ given as the average standard deviation between measured and calculated $\delta^{18}O_{SW}$ is 0.05 ‰. It was necessary to calculate $\delta^{18}O_{SW}$ from CTD salinity instead of using the measured $\delta^{18}O_{SW}$ to obtain continuous profiles. Results were converted from VSMOW to the VPDB scale by subtracting 0.27 ‰ [*Hut*, 1987]. Then, we applied a set of commonly used $\delta^{18}O$-temperature equations (Table 3) to predict equilibrium $\delta^{18}O_C$ using CTD temperature and the previously calculated $\delta^{18}O_{SW}$. Finally, we matched shell $\delta^{18}O$ to the $\delta^{18}O_C$ profiles. Since surface sediments were not always taken at the same positions as CTD, we matched shell $\delta^{18}O$ to profile(s) from those station(s), which are nearest to the core sites. To determine uncertainties of the calcification depth of each species and core site we estimated the calcification depths based on shell $\delta^{18}O$ with added/subtracted species-specific standard deviations. Depending on the standard deviation and the shape of the profiles, average uncertainties range between ±10 and 30 m.

CTD temperatures at depths corresponding to the estimated calcification depths give an estimate of the calcification temperatures for each species and core site. For *G. elongatus*, *P. obliquiloculata and N. dutertrei* only a few samples from the Philippines contained enough individuals to perform isotope analyses. For *G. tumida* none of the Philippines' samples contained enough specimens and therefore, depth and temperature estimates for this species are only representative for the area offshore PNG.

Table 3. General and species-specific $\delta^{18}O$-temperature equations used in this study

Reference	Species	Linear equations $T\ (°C) = a - b\ (\delta^{18}O_C - \delta^{18}O_{SW})$		
		a	b	
Bemis et al. [1998]	*O. universa (HL)*	14.9	-4.8	
Bouvier-Soumacnac and Duplessy [1985]	*N. dutertrei*	10.5	-6.58	
Farmer et al. [2007]	*G. ruber*	15.4	-4.78	
	G. sacculifer	16.2	-4.94	
	N. dutertrei	14.6	-5.09	
	P. obliquiloculata	16.8	-5.22	
	G. tumida	13.1	-4.95	
Mulitza et al. [2003]	*G. ruber*	14.2	-4.44	
	G. sacculifer	14.91	-4.35	
Shackleton [1974]	*Uvigerina sp.*	16.9	-4.0	
Spero et al. [2003]	*G. sacculifer*	12.0	-5.67	
		Quadratic equations $T(°C) = a - b\ (\delta^{18}O_C - \delta^{18}O_{SW}) + c\ (\delta^{18}O_C - \delta^{18}O_{SW})^2$		
		a	b	c
Kim and O'Neil [1997]	inorganic	16.1	-4.64	0.09

4. Results

4.1. Water column data and $\delta^{18}O_{SW}$-salinity regressions

The $\delta^{18}O_{SW}$-salinity relations for the study area during summer 2013 reveal that a $\delta^{18}O_{SW}$ increase of about 0.3 to 0.4 ‰ corresponds to a salinity increase of 1 psu (Figure 3). Regressions for surface waters offshore the Philippines and PNG (considering only samples from the Bismarck and Solomon Seas) are very similar (Figure 3a, blue and red dots, respectively). The regression line for surface waters offshore PNG shows only a slightly steeper slope and consequently, a smaller intercept. Taking all SO-228 and RR-1313 stations across the WPWP into account (Figure 3a, all black and colored dots) the surface $\delta^{18}O_{SW}$-salinity relation can be described as:

$$\delta^{18}O_{SW} = 0.37\ (\pm 0.03) * S - 12.4\ (\pm 1.0) \qquad (R^2 = 0.80) \qquad (I)$$

Regression lines describing the $\delta^{18}O_{SW}$-salinity relations for subsurface waters (NPTW and SPTW) show a shallower slope than for surface waters with slightly higher intercepts (Figure 3b). Due to the very small salinity ranges within the NPTW and SPTW it is difficult to assess a robust relationship for each of these water masses. The regressions also greatly depend on the depths and number of stations included in each equation. However, although NPTW and SPTW have different characteristics (see Figure 2), their $\delta^{18}O_{SW}$-salinity regressions are very similar to each other. Therefore, we also provide one equation for WPWP subsurface waters that includes all SO-228 and RR-1313 sample stations (Figure 3b, all black and colored dots).

$$\delta^{18}O_{SW} = 0.33\ (\pm 0.03) * S - 11.0\ (\pm 1.1) \qquad (R^2 = 0.67) \qquad (II)$$

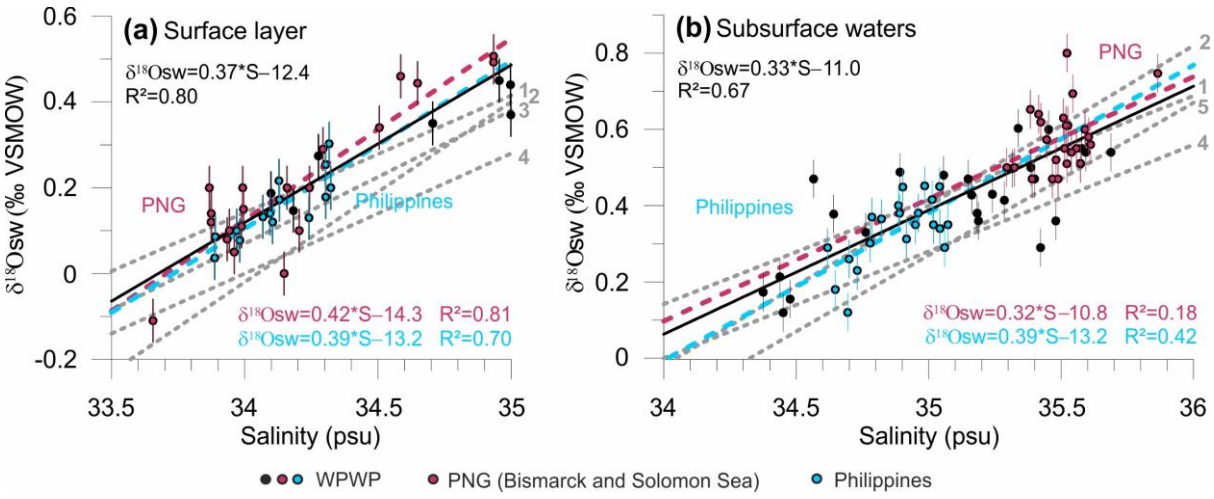

Figure 3. Regional $\delta^{18}O_{SW}$–salinity relations for (a) surface and (b) subsurface waters in the Western Pacific Warm Pool. Dots indicate individual samples included in the regressions. Red and blue colors indicate subsets of samples included in the regional regressions off Papua New Guinea (PNG) and the Philippines, respectively. Black dots indicate samples from sites that are not included in the regional regressions. Black lines indicate regression lines for the entire study area and colored lines for the subareas. Gray stippled lines show regional δ^{18}Osw–salinity equations published by 1. *Fairbanks et al.* [1997], 2. *Morimoto* [2002], 3/5. *Leech et al.* [2013], 4. [*LeGrande and Schmidt*, 2011]. Bars indicate laboratory standard deviations for oxygen isotope measurements.

4.2. Calcification depth

In general, shell δ^{18}O increases with increasing calcification depth of the species. *G. ruber* and *G. elongatus* record the lowest δ^{18}O values and *G. tumida* records the highest δ^{18}O values. *G. sacculifer*, *P. obliquiloculata* and *N. dutertrei* calcify in between. Shell δ^{18}O and our derived mean calcification depths of the species used are very similar offshore the Philippines and PNG. Therefore, in our discussion we do not distinguish between samples from the Philippines and PNG. Figure 4 and Table 4 give δ^{18}O-derived depths for all species as estimated by applying the δ^{18}O-temperature equation of *Bemis et al.* [1998]. Depth estimates for each species applying different δ^{18}O-temperature equations in comparison are provided in the supplementary information (Figures S4–6).

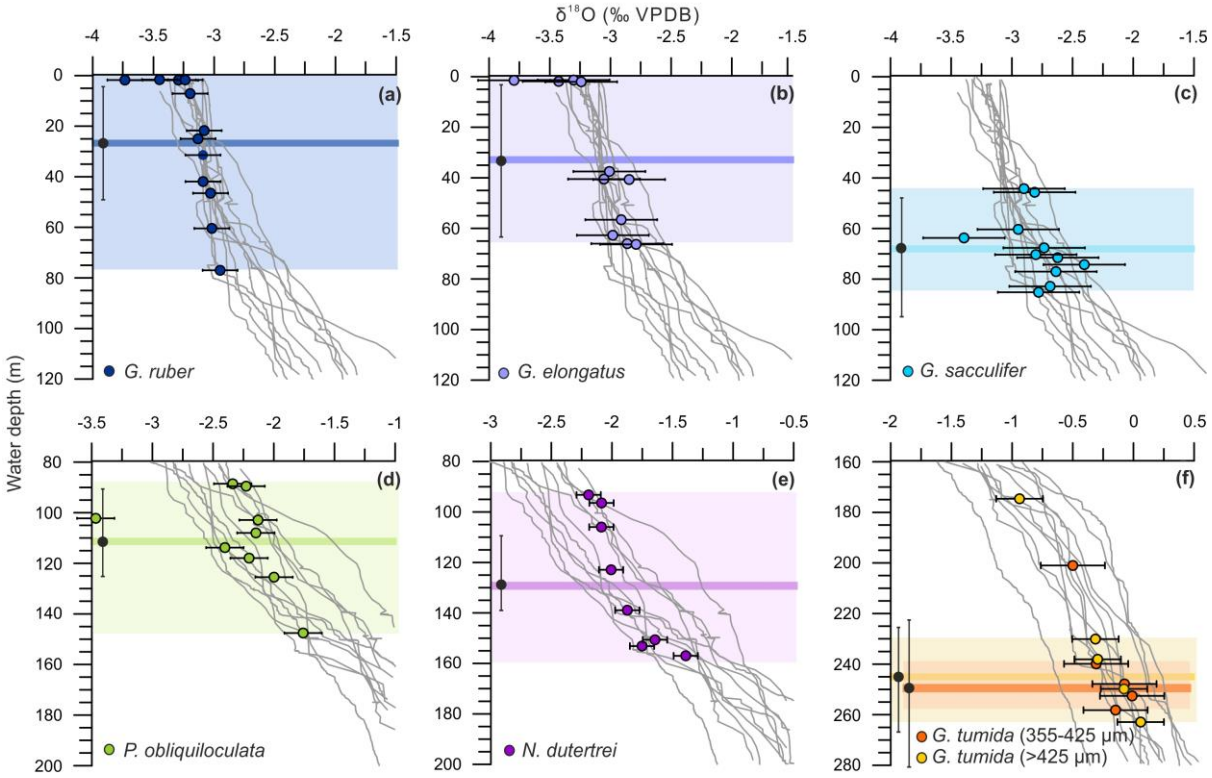

Figure 4. Shell $\delta^{18}O$ derived calcification depth estimates for several planktic foraminifera (colored dots) in the Western Pacific Warm Pool. Gray lines indicate depth profiles of predicted $\delta^{18}Oc$ calculated from individual CTD casts (see section 3.5 for details). The average calcification depth at each core site is determined by matching shell $\delta^{18}O$ to $\delta^{18}O_C$ of the profile(s) nearest to the respective core site. Horizontal bars indicate species-specific standard deviations for shell $\delta^{18}O$, vertical bars on black dots show exemplarily average uncertainties in calcification depth derived by projecting shell $\delta^{18}O$ with added/subtracted standard deviations on the $\delta^{18}O_C$ profiles. The uncertainty of the $\delta^{18}O_C$ profiles arising from the average standard deviation between measured and calculated $\delta^{18}O_{SW}$ is 0.05 ‰ (not shown). Colored shading indicates calcification depth ranges for the individual species in the study area. The average calcification depth is highlighted by colored horizontal bars. Note the different scaling of the axes in different panels. Individual data points, which are shown outside the range of predicted $\delta^{18}O_C$ do not match any profile (see text).

Table 4. Calcification depth and temperatures. The calcification depth of each species and core site was estimated by comparing shell $\delta^{18}O$ to depth profiles of predicted $\delta^{18}O$ calcite. Predicted $\delta^{18}O_C$ was calculated from CTD salinity applying the $\delta^{18}O_{SW}$-salinity equations of this study and the $\delta^{18}O$-temperature equation of *Bemis et al.* [1998] using CTD temperature. We assigned a depth of 0 m to samples that did not match any profile. Calcification temperatures are CTD temperatures at depth corresponding to the estimated calcification depths.

Core	*G. ruber* (250-355 µm)		*G. elongatus* (250-355 µm)		*G. sacculifer* (250-355 µm)		*P. obliquiloculata* (355-425 µm)		*N. dutertrei* (355-425 µm)		*G. tumida* (355-425 µm)		*G. tumida* (>425 µm)	
	Depth (m)	Temp. (°C)	Depth (m)	Temp. (°C)	Depth (m)	Temp. (°C)	Depth (m)	Temp. (°C)	Depth (m)	Temp. (°C)	Depth (m)	Temp. (°C)	Depth (m)	Temp. (°C)
Philippines														
RR1313-24 50MC	7	29.8	0	29.6	85	28.4	0	29.8	140	24.3	-	-	-	-
RR1313-25 53MC	77	28.3	0	28.8	-	-	-	-	-	-	-	-	-	-
GeoB 17404-2	47	28.9	57	28.5	83	27.8	-	-	-	-	-	-	-	-
GeoB 17410-3	22	29.3	0	29.9	70	28.2	-	-	-	-	-	-	-	-
GeoB 17414-2	25	29.2	37	28.7	45	28.2	88	25.8	94	25.3	-	-	-	-
Papua New Guinea														
GeoB 17419-2	32	29.7	40	29.8	60	29.6	147	24.6	150	24.2	200	18.8	175	20.9
RR1313-12 30MC	0	29.7	-	-	0	29.7	114	27.5	-	-	-	-	-	-
GeoB 17421-2	0	29.7	0	29.7	77	28.3	117	26.7	157	23.1	240	17.7	-	-
GeoB 17429-1	60	29.0	67	28.6	72	27.9	125	25.8	123	25.8	248	16.4	250	15.9
GeoB 17430-2	42	29.2	63	28.7	68	28.5	108	26.3	153	24.7	252	15.8	230	17.6
GeoB 17432-3	0	29.4	66	28.6	75	27.5	103	26.2	107	26.0	-	-	263	15.6
GeoB 17435-2	0	28.9	40	28.9	45	26.7	90	26.9	97	26.2	258	16.6	238	17.7

4.2.1. Mixed layer species: *G. ruber, G. elongatus* and *G. sacculifer*

Average shell $\delta^{18}O$ values are very similar for *G. ruber* and *G. elongatus* (-3.19 and -3.11 ‰, Table 1). This implies very similar calcification depths for both species in the WPWP. Depending on the selected $\delta^{18}O$-temperature equation, shell $\delta^{18}O$ derived mean calcification depths range from 0 to 45–105 m (Figures 4 and S4). Applying the $\delta^{18}O$-temperature equations of *Bemis et al.* [1998] and *Shackleton* [1974] the estimated depth range is within the upper 80 m of the water column for both, *G. ruber* and *G. elongatus*. By applying the equations of *Kim and O'Neil* [1997] and *Farmer et al.* [2007] calcification depths shoal to 0–45 m and 0–65 m, respectively, while the application of the species-specific equation of *Mulitza et al.* [2003] result in a slightly deeper depth range (0–105 m) (Figure S5a).

Shell $\delta^{18}O$ of *G. sacculifer* varies around -2.73 ‰ (excluding RR1313-12 30MC) (Table 1). Applying different $\delta^{18}O$-temperature equations, the mean calcification depth varies between 45 and 95 m. It ranges from 45 to 85 m using the equation of *Bemis et al.* [1998] (Figure 4c) and from 55 to 95 m applying the $\delta^{18}O$-temperature equations of *Shackleton* [1974] and *Spero et al.* [2003]. The equations of *Farmer et al.* [2007] and *Kim and O'Neil* [1997] lead to slightly shallower calcification depths (0–70 m) and the equation of *Mulitza et al.* [2003] to deeper calcification depths (70–110 m) (Figure S5b). Note that sample RR1313-12 30MC shows an extremely low $\delta^{18}O$ value (-3.39 ‰), which does not match any profile.

4.2.2. Upper thermocline species: *P. obliquiloculata* and *N. dutertrei*

Shell $\delta^{18}O$ of *P. obliquiloculata* varies around -2.15 ‰ (excluding RR1313-24 50MC) (Table 1). For the majority of the samples this indicates a calcification depth between 90 and 125 m when applying the $\delta^{18}O$-temperature equation of *Bemis et al.* [1998] (Figure 4d). Applying the equations of *Shackleton* [1974] or *Bouvier-Soumagnac and Duplessy* [1985] leads to very similar calcification depths (85–120 and 90–130 m), the equations of *Kim and O'Neil* [1997] and *Farmer et al.* [2007] leads to slightly shallower calcification depths (70-105 and 40-75 m) (Figure S6a). Our foraminifera tests from site GeoB 17419-2 record exceptionally high $\delta^{18}O$ values resulting in, compared to the other core sites, relatively deeper (20–40 m) calcification depths. With a $\delta^{18}O$ value of -3.47 ‰ (Table 1), sample RR1313-24 50MC does not match any $\delta^{18}O_C$ profile.

447 The *N. dutertrei* average shell $\delta^{18}O$ of -1.88 ‰ is slightly higher than that of *P. obliquiloculata*.
448 By using the equations of *Bemis et al.* [1998], *Shackleton* [1974] or *Farmer et al.* [2007] shell
449 derived calcification depths vary between around 90 and 160 m (Figures 4e and S5b). The
450 application of the $\delta^{18}O$-temperature equation from *Kim and O'Neil* [1997] or *Bouvier-*
451 *Soumagnac and Duplessy* [1985] result in slightly shallower or deeper depth ranges (80–150
452 or 95–155 m) (Figure S6b).
453

454 4.2.3. Lower thermocline species: *G. tumida*

455 Average shell $\delta^{18}O$ of *G. tumida* is -0.15 ‰ for the 355–425 µm size fraction and -0.14 ‰ for
456 the >425 µm size fraction (excluding GeoB 17419-2) (Table 1). Shell $\delta^{18}O$ of individual
457 samples differ by maximal 0.3 ‰. Hence, under the restriction of the small set of samples, our
458 data indicate, that there is no major size effect on the calcification depths of *G. tumida*. Based
459 on the equation of *Bemis et al.* [1998] the calcification depth of *G. tumida* at most sites is
460 between 230 and 265 m water depth (Figure 4f). The application of the equations from
461 *Shackleton* [1974] and *Kim and O'Neil* [1997] results in slightly shallower calcification depths,
462 ranging between 195 and 235 m. Based on the species-specific equation of *Farmer et al.* [2007]
463 the estimated calcification depths are slightly deeper, ranging between 255 and 310 m (Figure
464 S7). Exceptionally low $\delta^{18}O$ in *G. tumida* shells from GeoB 17419-2 indicates up to 70 m
465 shallower calcification depth at this site, independent of the size fraction used.
466

467 4.3. Shell Mg/Ca

468 Mg/Ca ratios recorded in the Philippines and PNG samples are very similar. *G. ruber* and *G.*
469 *elongatus* record highest Mg/Ca, averaging 5.26 and 5.37 mmol/mol, respectively. Shell
470 Mg/Ca in *G. sacculifer* varies around 3.85 mmol/mol. *N. dutertrei* and *P. obliquiloculata* show
471 similar shell Mg/Ca varying around 2.60 and 2.66 mmol/mol, respectively. *G. tumida* shows
472 lowest Mg/Ca ratios around 1.88 mmol/mol (355–425 µm) and 1.69 mmol/mol (>425 µm).
473 Hence, average Mg/Ca of the different species confirms the results obtained from oxygen
474 isotope ratios with calcification depths being shallowest for *G. ruber*, *G. elongatus* and *G.*
475 *sacculifer*, intermediate for *P. obliquiloculata* and *N. dutertrei* and deepest for *G. tumida*.
476 Mg/Ca ratios of *P. obliquiloculata* in RR1313-24 50MC, *N. dutertrei* in RR1313-53MC, and
477 *G. tumida* in GeoB 17410-3 are exceptionally high (3.17 mmol/mol, 4.23 mmol/mol, and 3.27
478 mmol/mol) (Table 1). The high Mg/Ca value of *P. obliquiloculata* in RR1313-24 50MC goes

along with exceptionally low $\delta^{18}O$ and could therefore indicate an extremely shallow calcification depth at this site. Due to the limited number of specimens of *N. dutertrei* in RR1313-25 53MC and *G. tumida* in GeoB 17410-3, we could not measure the oxygen isotope composition in these samples.

5. Discussion

5.1. Water column data and $\delta^{18}O_{SW}$-salinity regressions

Generally, our surface and subsurface $\delta^{18}O_{SW}$-salinity regressions are within the range of published WPWP regressions [*Fairbanks et al.*, 1997; *Leech et al.*, 2013; *LeGrande and Schmidt*, 2011; *Morimoto*, 2002]. However, slope and/or intercept differ from previous regression lines. Especially the regressions of *Fairbanks et al.* [1997], *LeGrande and Schmidt* [2011] and the surface regression of *Leech et al.* [2011] show shallower slopes (around 0.3) and accordingly, larger intercepts (between -10.47 and -9.14) than our regressions. The regression of *Morimoto et al.* [2002] is almost identical to our PNG surface equation ($\delta^{18}O_{SW}$ = 0.42*S-14.3). Since $\delta^{18}O_{SW}$-salinity relations depend on local environmental conditions, deviations are most probably due to different sampling sites, water depths and periods.

For the first time, we generated equations for individual water masses (surface waters, NPTW and SPTW). Our results reveal that for both, WPWP wide and regional regressions, the ratio between $\delta^{18}O_{SW}$ and salinity is higher in surface than in subsurface waters. Therefore, it appears reasonable to use different $\delta^{18}O_{SW}$-salinity regressions for surface and subsurface water masses. The regression coefficients of our regression lines (Figure 3) indicate that the application of a more general, WPWP wide regression for combined NPTW and SPTW is more robust than individual regressions for the NPTW and SPTW. This is due to the very small salinity range within the NPTW offshore the Philippines and the SPTW offshore PNG.

5.2. Calcification depths and temperatures

Accurate calcification depth estimates are indispensable to deduce precise calcification temperatures for each species. The accuracy of the depth estimates depends on the precision of the $\delta^{18}O_{SW}$-salinity equation applied, the choice of the $\delta^{18}O$-temperature equation, the availability of local water column data, the seasonal and interannual variations in local

hydrography and possible shell disequilibrium effects [see *Regenberg et al.*, 2009; *Steph et al.*, 2009].

A comparison between predicted $\delta^{18}O_C$ calculated using discrete $\delta^{18}O_{SW}$ measured in water samples and predicted $\delta^{18}O_C$ using $\delta^{18}O_{SW}$ calculated from CTD salinity shows that the calculated values reproduce measured $\delta^{18}O$ precisely (Figure S8). The average deviation between calculated and measured $\delta^{18}O_{SW}$ is ±0.07 ‰, the maximal deviation is ±0.35 ‰ and only 6 out of 98 samples yielded $\delta^{18}O_{SW}$ differences larger than 0.20 ‰ (see Table S2). The comparison provides reliability to the accuracy of the $\delta^{18}O_{SW}$-salinity equations for our sampling period and sites.

For the following analyses we use calcification depth estimates based on the $\delta^{18}O$-temperature equation that was generated by *Bemis et al.* [1998] in a culture experiment for *O. universa*. Although it has been obtained on a single species not used in our study, this equation is commonly used for other planktic foraminiferal species [e.g. *Mohtadi et al.*, 2014; *Spero et al.*, 2003; *Thunell et al.*, 1999] and its application gives realistic results for all species used here. The equations of *Shackleton* [1974], *Bouvier-Soumagnac and Duplessy* [1985], and *Spero et al.* [2003] lead to similar calcification depths. The quadratic equation of *Kim and O'Neil* [1997] results in marginally shallower depths for surface and similar depths for subsurface dwellers. The application of the equations of *Farmer et al.* [2007] result in slightly shallower calcification depths. The equations of *Farmer et al.* [2007] are based on sample material from much greater water depths (mostly 3000-4000 m) where carbonate is affected by dissolution [*Hertzberg and Schmidt*, 2013] which would increase $\delta^{18}O$ in foraminiferal tests. Consequently, the application of these equations would underestimate calcification depths. The equations proposed by *Mulitza et al.* [2003] result in deeper calcification depths. These equations are based on plankton tow studies and might overestimate calcification depths due to lower $\delta^{18}O$ in shells of living foraminifera [see *Regenberg et al.*, 2009 and references therein].

Based on the assumption that planktic foraminifera calcify perennially in the WPWP we assume that our $\delta^{18}O$ data represent mean annual conditions. However, we note that data from individual samples might be biased and reflect other than normal conditions (e.g. a single season or El Niño/La Niña conditions). We are well aware that our hydrographic data show a snapshot and therefore, do not necessarily represent mean annual hydrography. However,

seasonal temperature and salinity variations are very small in our study area and mostly restricted to the mixed layer (see section 2). Interannual variations in ocean hydrography are mainly caused by ENSO variability. Our water column data were collected during a normal year and are thus, not biased to El Niño or La Niña conditions. Considering the paucity of continuous subsurface temperature, salinity and especially $\delta^{18}O_{SW}$ data from the WPWP, our work provides the first simultaneous measurements on these parameters at different water depths at stations in close proximity to our core sites and thus, the hitherto most suitable hydrographic estimates for the determination of calcification depths and temperatures.

Nonetheless, we also compared shell $\delta^{18}O$ with depth-profiles of $\delta^{18}O_C$ calculated by using mean annual temperature and salinity data from the World Ocean Atlas 13 (WOA13) [*Locarnini et al.*, 2013; *Zweng et al.*, 2013]. Shell $\delta^{18}O$ of most *G. ruber* and *G. elongatus* samples do not match the WOA13 $\delta^{18}O_C$ profiles. WOA13 derived calcification depths of *G. sacculifer* extent over a larger depth range than SO-228 and RR-1313 CTD (from here on referred to as CTD) calcification depths. WOA13 depth estimates of *P. obliquiloculata, N. dutertrei* and *G. tumida* differ only slightly from CTD derived depth estimates (maximal 35 m) with a tendency to shallower depths. Overall, for our study, the application of CTD data gives more realistic results than the application of WOA13 data.

Previous studies have shown that many species do not calcify in isotopic equilibrium with seawater [see *Ravelo and Hillaire-Marcel*, 2007 and references therein]. Potential reasons are the photosynthetic activity of symbionts, incorporation of low $\delta^{18}O$ metabolic CO_2, species-specific calcification rates, the addition of gametogenic calcite, and possibly carbonate ion concentrations of the ambient seawater [see *Ravelo and Hillaire-Marcel*, 2007 and references therein]. Disequilibrium effects depend on local conditions and the sample material used. For most species used in our study, negative disequilibrium effects ranging between 0.0 and 1.0 ‰ are presumed [see *Lončarić et al.*, 2006; *Niebler et al.*, 1999 and references therein]. No vital effects are reported for *G. tumida.* Correcting for negative disequilibrium effects would increase shell $\delta^{18}O$, and subsequently result in deeper calcification depths and colder calcification temperatures [see discussion in *Regenberg et al.*, 2009]. However, the large variety of factors that could possibly influence shell $\delta^{18}O$ makes it difficult to correct $\delta^{18}O$ for disequilibrium effects precisely. In addition, most published $\delta^{18}O$-temperature equations do not take into account biological disequilibrium effects on $\delta^{18}O$. Therefore, we did not correct $\delta^{18}O$ values for disequilibrium effects.

Overall, our results show that *G. ruber* and *G. elongatus* calcify within the mixed layer (0–80 m) and *G. sacculifer* calcifies at the bottom of the mixed layer (45–85 m). *P. obliquiloculata* and *N. dutertrei* calcify within the upper thermocline, whereby our $\delta^{18}O$ values indicate that *N. dutertrei* calcifies within a larger depth range (90-160 m) than *P. obliquiloculata* does (90-125 m). *G. tumida* seems to calcify well below *P. obliquiloculata* and *N. dutertrei* within the lower thermocline at depth between 230 and 265 m. In relation to water masses, this means that *G. ruber*, *G. elongatus* and *G. sacculifer* calcify in surface waters. *P. obliquiloculata*, and *N. dutertrei* calcify predominantly within the NPTW offshore the Philippines and within the SPTW offshore PNG. *G. tumida* calcifies within the transition between NPTW/SPTW and NPIW or AAIW. Our depth estimates generally agree with results from sediment traps and plankton tows in the central equatorial Pacific, North Pacific and Indian Oceans [*Kuroyanagi and Kawahata*, 2004; *Mohtadi et al.*, 2009; *Peeters et al.*, 2002; *Rippert et al.*, 2016; *Watkins et al.*, 1996]. However, our data show a tendency to somewhat deeper absolute calcification depths and wider depth ranges for most species, probably owing to a generally thick mixed layer and deep thermocline in the WPWP. Recent results from the eastern WPWP indicate even deeper habitat depths of planktic foraminifera [*Rippert et al.*, 2016]. Such differences in absolute calcification depths are likely related to the specific regional hydrographic conditions in each study area. For *G. ruber* and *G. elongatus,* our data imply very similar calcification depths. This is in sharp contrast to studies from the South China Sea and North Pacific Ocean that suggest a deeper habitat depth for *G. elongatus* [*Kawahata*, 2005; *Steinke et al.*, 2005; *Wang*, 2000] but in agreement with studies from the eastern Indian Ocean and the Caribbean Sea, which suggest the same habitat depth for both species [*Mohtadi et al.*, 2009; *Thirumalai et al.*, 2014].

5.3. Mg/Ca versus calcification temperatures

A large number of studies revealed that Mg/Ca in planktic foraminiferal tests show an exponential relationship with ocean temperatures [e.g. *Anand et al.*, 2003; *Cléroux et al.*, 2008; *Dekens et al.*, 2002; *Elderfield and Ganssen*, 2000; *McConnell and Thunell*, 2005; *Mohtadi et al.*, 2009; *Mohtadi et al.*, 2011; *Nürnberg et al.*, 1996; *Regenberg et al.*, 2009]. Some culture and core top studies also described a positive salinity effect on shell Mg/Ca of planktic foraminifera [*Arbuszewski et al.*, 2010; *Ferguson et al.*, 2008; *Kısakürek et al.*, 2008; *Mathien-Blard and Bassinot*, 2009; *Nürnberg et al.*, 1996]. However, studies suggesting a significant

salinity influence have been criticized due to substantial dissolution effects, seasonality [*Arbuszewski et al.*, 2010] or diagenetic alteration [*Ferguson et al.*, 2008] on the sample material [*Hertzberg and Schmidt*, 2013; *Hönisch et al.*, 2013]. However, in our study area the salinity range is rather small (between 33.9 and 35.6 psu). Variations between stations at water depths that correspond to the calcification depth of individual foraminifera species at the corresponding core sites are below 1.2 psu. There is no significant correlation between Mg/Ca and salinity (R-values range between 0.00 and 0.35 for individual species). Besides, shell Mg/Ca in samples from offshore the Philippines and PNG are very similar, although these areas are influenced by water masses characterized by different salinities (Figure 2). Therefore, we argue that shell Mg/Ca in our samples is not biased by salinity. Some studies also indicate a negative effect of pH or [CO_3^{2-}] on Mg/Ca [*Evans et al.*, 2016; *Kısakürek et al.*, 2008; *Lea et al.*, 1999; *Russell et al.*, 2004; *Spero et al.*, 2015]. To date, it is not clear whether pH or [CO_3^{2-}] exert a dominant control on Mg/Ca [*Allen et al.*, 2016; *Evans et al.*, 2016]. Moreover, the effect is neither constant over temperature [*Spero et al.*, 2015], nor the same for different planktic foraminifera species [e.g. *Allen et al.*, 2016] and some studies provide confidence that the effect is negligible for ambient seawater conditions [*Kısakürek et al.*, 2008; *Russell et al.*, 2004]. Since pH or [CO_3^{2-}] were not measured during both SO-228 and RR-1313 expeditions, we cannot estimate the range of these parameters over the study area. We do not apply any corrections for possible effects of carbonate chemistry on shell Mg/Ca, while we cannot fully exclude such effect on our samples. More extensive culture and/or sediment trap studies are required to quantify the effect pH or [CO_3^{2-}] on Mg/Ca of the various planktic foraminifera species.

Mg/Ca to temperature calibrations are usually expressed as Mg/Ca = B exp (A*Temperature). We combined data of all species and compared shell Mg/Ca to CTD temperature at $\delta^{18}O$-derived calcification depths in a multispecies approach (Figure 5). A depth of 0 m was assigned to samples, where shell $\delta^{18}O$ did not match the $\delta^{18}O_C$. Mg/Ca and temperature show a clear exponential relationship (Figure 5). Previous studies suggest that this relationship is best described by a reduced major axis (or geometric mean) regression (RMA) of the natural Log of (Mg/Ca) against calcification temperature [*Anand et al.*, 2003; *Rosenthal and Lohmann*, 2002]. An advantage of the RMA is that it accounts for both, uncertainties in Mg/Ca and calcification temperatures. Especially in field studies, calcification temperatures inherit an intrinsic scatter that arises from a range of different factors including uncertainties in the depth estimates or seasonality for example.

Using the RMA approach, the multispecies Mg/Ca-temperature relation is described by the following equation:

$$Mg/Ca = 0.26\ (\pm 0.04)\ \exp\ 0.097*T\ (\pm 0.006) \qquad \text{(III)}$$

The calculation followed *Isobe et al.* [1990]. The uncertainties of the slope and intercept are given as standard deviations assuming that the intrinsic scatter of the data dominates any errors of the measurement process.

For comparison, we also calibrated shell Mg/Ca against WOA13 mean annual temperatures. Despite the differences in estimated calcification depths, WOA13 derived calcification temperatures are very similar to CTD derived calcification temperatures. The reason is that temperatures of the WOA13 climatology are generally lower than our CTD temperatures at the same depth levels. Due to the similarity of the calcification temperatures, the WOA13 derived regression is within the error range of the regression based on CTD derived calcification temperatures. (A = 0.101, B = 0.24).

Our multispecies Mg/Ca-temperature relation is in good agreement with previously published multispecies and species-specific temperature calibrations (Figure 5 and Table 5). However, comparing our calibration to published ones, it has to be noted that our calibration is based on samples that were treated by reductive cleaning, whereas most published calibrations are based on samples cleaned without a reductive step. Previous studies indicate that the reductive cleaning leads to a decrease in Mg/Ca [e.g. *Barker et al.*, 2003; *Xu et al.*, 2010]. To estimate the effects on the Mg/Ca-temperature relations, we applied a correction assuming that the Mg/Ca relations were reduced by about 10 % in all samples [e.g. *Barker et al.*, 2003; *Martin and Lea*, 2002; *Rosenthal et al.*, 2004]. We note that some studies suggest different values for individual species [e.g. *Xu et al.*, 2010], but since exact rates of Mg/Ca loss are unknown for most species, we presume a constant rate of 10 % for all species. The resulting regression line shows the same slope as the original calibration (0.097), and an only slightly modified intercept (0.24). Thus, the modified calibration is within the error range of the original one.

A multispecies equation does not seem accurate enough to describe the Mg/Ca-temperature relation of individual species in the WPWP. For example, all the *G. ruber* and *G. elongatus* samples fall above, and all the *P. obliquiloculata* and *N. dutertrei* samples fall below the

679 regression line. That means, calcification temperatures of *G. ruber* and *G. elongatus* are
680 overestimated, and those of *P. obliquiloculata* and *N. dutertrei* are underestimated by the
681 multispecies regression. For that reason, species-specific regression lines are additionally
682 required to reconstruct calcification temperatures for individual species precisely. Since the
683 temperature range between the sites in our study area is very narrow, it is difficult to determine
684 the temperature sensitivity for individual species unequivocally. Hence, we calculated regional
685 species-specific regressions by assuming the same temperature sensitivity, A = 0.097, as it was
686 calculated by the multispecies approach, for all species (Figure 5). The resulting regression
687 lines for *G. ruber* and *G. elongatus* are very similar to the multispecies and species-specific
688 regression published by *Anand et al.* [2003] or *Dekens et al.* [2002], respectively (Mg/Ca =
689 0.39 exp 0.09*T). For the temperature range relevant for this study the regression lines of *G.*
690 *tumida* fall next to the multispecies regression lines of *Anand et al.* [2003] and *Sagawa et al.*
691 [2012]. However, especially slope and intercept of the *Sagawa et al.* [2012] regression differ
692 from those of our species-specific regression (Table 5) and it is important to note that the slope
693 affects the amplitude of temperature variations in paleorecords. The regression lines of *G.*
694 *sacculifer*, *P. obliquiloculata* and *N. dutertrei* deviate from previously published correlations
695 (Figure 5). Calcification temperatures of these species are exceptionally warm in the western
696 tropical Pacific Ocean despite deeper calcification depths and thus, *G. sacculifer*, *P.*
697 *obliquiloculata* and *N. dutertrei* require regional, species-specific Mg/Ca-temperature
698 calibrations. Assuming the temperature sensitivity calculated by the multispecies approach (A
699 = 0.097) our data indicate an intercept of B = 0.24 for *G. sacculifer* and an intercept of B =
700 0.21 for both *P. obliquiloculata* and *N. dutertrei* (Figure 5).
701

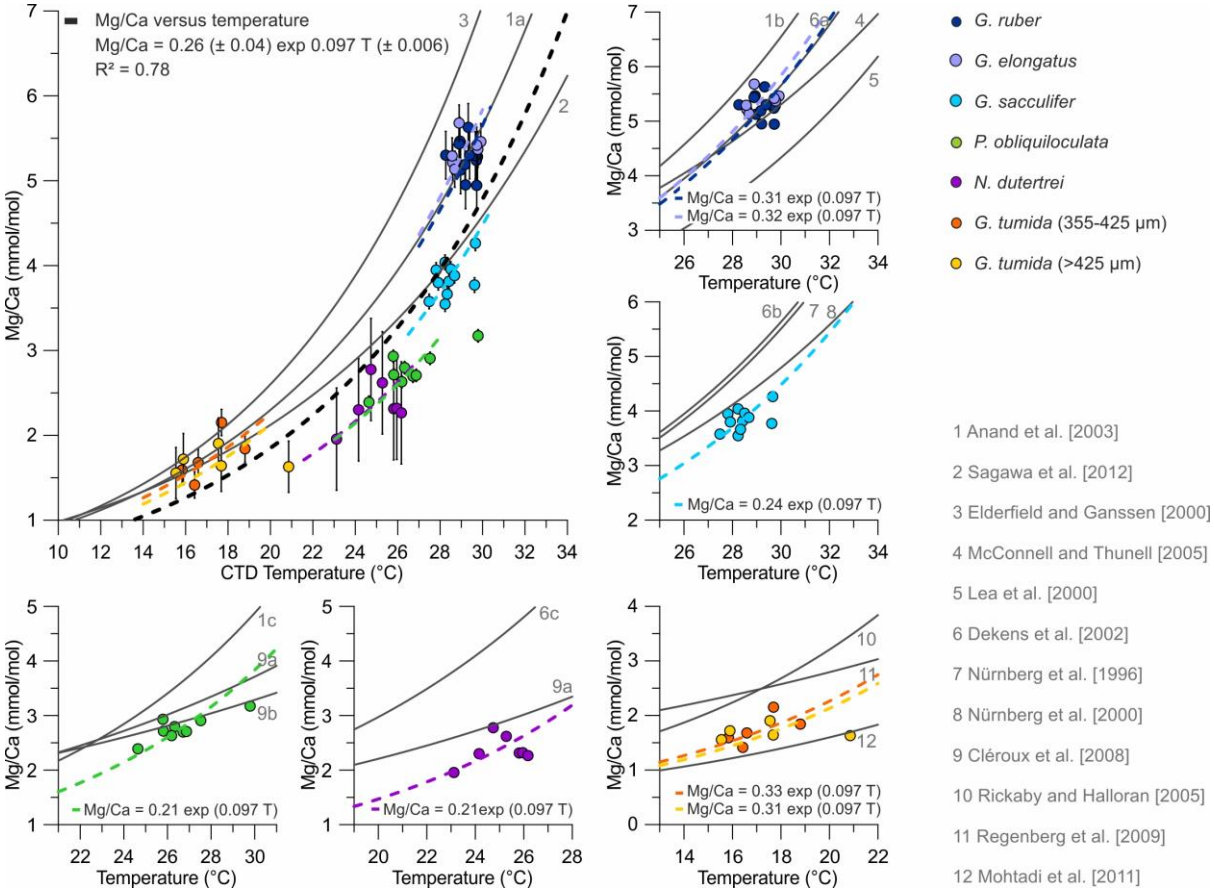

Figure 5. Shell Mg/Ca versus calcification temperature for different planktic foraminifera species. Black bars indicate species-specific standard deviations of Mg/Ca. Black and colored dashed lines indicate regional multispecies and species-specific regressions calculated with a RMA regression (this study). Gray solid lines show published multispecies (large graph) and species-specific (small graphs) regression lines. Numbers denote published calibrations (see also table 5). Note that a, b and c refer to different calibrations in the same publication.

Table 5. Multispecies and species-specific Mg/Ca temperature in comparison to previously published relations. Calibration numbers introduced in figure 5 are given in gray.

Reference	Species	Exponential relation Mg/Ca = B exp (A*Temperature)	
		A	B
Anand et al. [2003] (1a)	multispecies	0.09	0.38
Sagawa et al. [2011] (2)	multispecies	0.077	0.455
Elderfield and Ganssen [2000] (3)	multispecies	0.1	0.352
This study	multispecies	0.097	0.26
Anand et al. [2003] (1b)	*G. ruber*	0.09	0.44
McConnell and Thunell [2005] (4)	*G. ruber*	0.068	0.69

Lea et al. [2000] (5)	*G. ruber*	0.089	0.3
Dekens et al [2002] (6a)	*G. ruber*	0.09	0.38
This study	*G. ruber*	0.097	0.31
This study	*G. elongatus*	0.097	0.32
Dekens et al. [2002] (6b)	*G. sacculifer*	0.09	0.37
Nürnberg et al. [1996] (7)	*G. sacculifer*	0.089	0.39
Nürnberg et al. [2000] (8)	*G. sacculifer*	0.076	0.49
This study	*G. sacculifer*	0.097	0.24
Anand et al. [2003] (1c)	*P. obliquiloculata*	0.09	0.328
Cléroux et al. [2008] (9b)	*P. obliquiloculata*	0.039	1.02
This study	*P. obliquiloculata*	0.097	0.21
Dekens et al. [2002] (6c)	*N. dutertrei*	0.08	0.6
This study	*N. dutertrei*	0.097	0.21
Cléroux et al. [2008] (9a)	Deep dwelling species	0.052	0.78
Rickaby and Halloran [2005] (10)	*G. tumida*	0.09	0.53
Regenberg et al. [2009] (11)	*G. tumida*	0.041	1.23
Mohtadi et al. [2011] (12)	*G. tumida*	0.068	0.41
This study	*G. tumida* (355-425 µm)	0.097	0.33
This study	*G. tumida* (>425 µm)	0.097	0.31

A comparison of Mg/Ca-temperatures and calcification temperatures gives a measure of the uncertainty inherent in the Mg/Ca-temperature calibrations [*Anand et al.*, 2003]. We compared Mg/Ca-temperatures calculated by the application of species-specific calibrations to $\delta^{18}O$-derived calcification temperatures (Figure 6). The average standard error between Mg/Ca and $\delta^{18}O$-derived calcification temperatures is 0.5°C. The consistency of Mg/Ca and $\delta^{18}O$-derived calcification temperatures validates our previous steps and assumptions, and gives further evidence, that Mg/Ca and $\delta^{18}O$ data are not influenced by secondary effects.

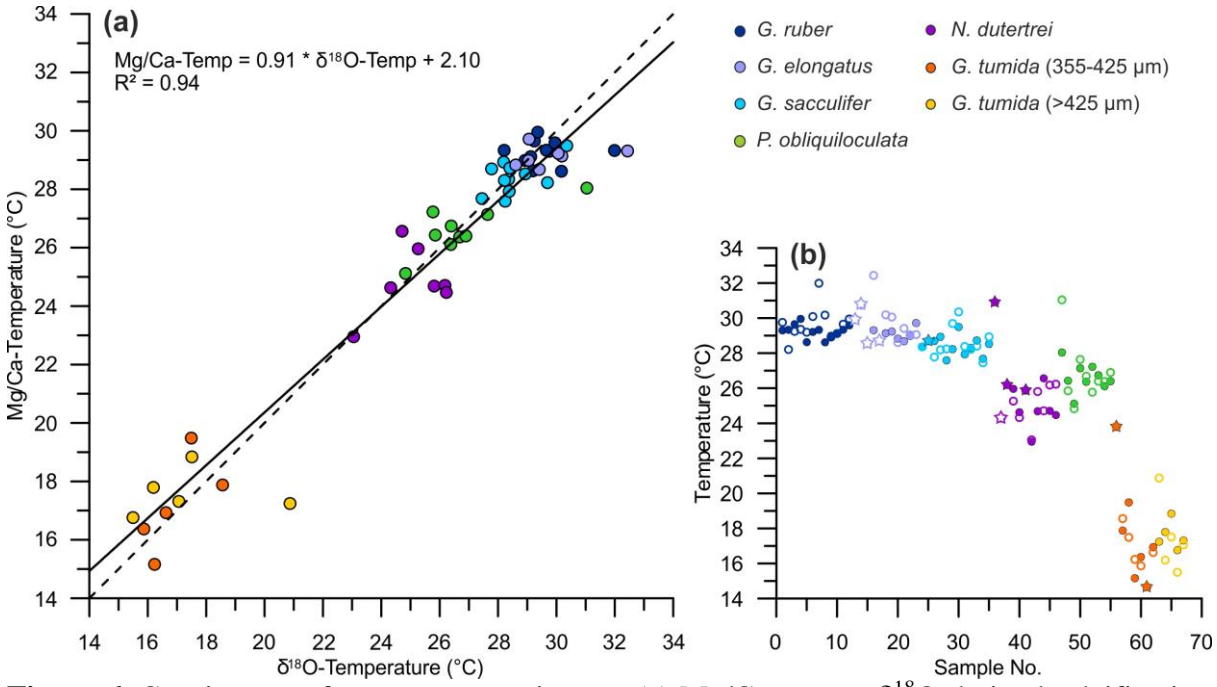

Figure 6. Consistency of temperature estimates. (a) Mg/Ca- versus $\delta^{18}O$-derived calcification temperatures. Mg/Ca-temperatures are based on species-specific regressions; $\delta^{18}O$-temperatures were calculated with the equation of *Bemis et al.* [1998]. The black solid line shows the correlation between Mg/Ca- and $\delta^{18}O$-temperatures. For comparison, the 1:1 relationship is shown (stippled line). (b) Comparison of Mg/Ca-temperatures (filled symbols) and $\delta^{18}O$-temperatures (open symbols). Note that (a) includes only samples with paired $\delta^{18}O$ and Mg/Ca measurements, whereas (b) includes all samples where $\delta^{18}O$ or Mg/Ca measurements are available. Samples where only $\delta^{18}O$ or Mg/Ca measurements are available are marked with stars. Sample numbers are related to cores as defined in Table S3.

5.4. Application of our Mg/Ca-temperature regression

Our species-specific equations were applied to convert Mg/Ca into temperature (Figure 7). While our regional Mg/Ca to temperature relations were established on the basis of only samples for which we have $\delta^{18}O$ measurements and thereby direct estimates of foraminiferal calcification depths at the respective core site, we applied the equations to all samples where we measured Mg/Ca ratios (see. Table 1). Temperatures obtained from *G. ruber* and *G. elongatus* match mixed layer temperatures. Mg/Ca temperatures of *G. sacculifer* correspond to temperatures from the mixed layer bottom and uppermost thermocline. Mg/Ca temperatures calculated from *P. obliquiloculata* and *N. dutertrei* reflect upper and those calculated from *G. tumida* lower thermocline conditions. *P. obliquiloculata* and *N. dutertrei* are most suitable to

track changes in NPTW and SPTW since they calcify at water depths corresponding to the core of these water masses.

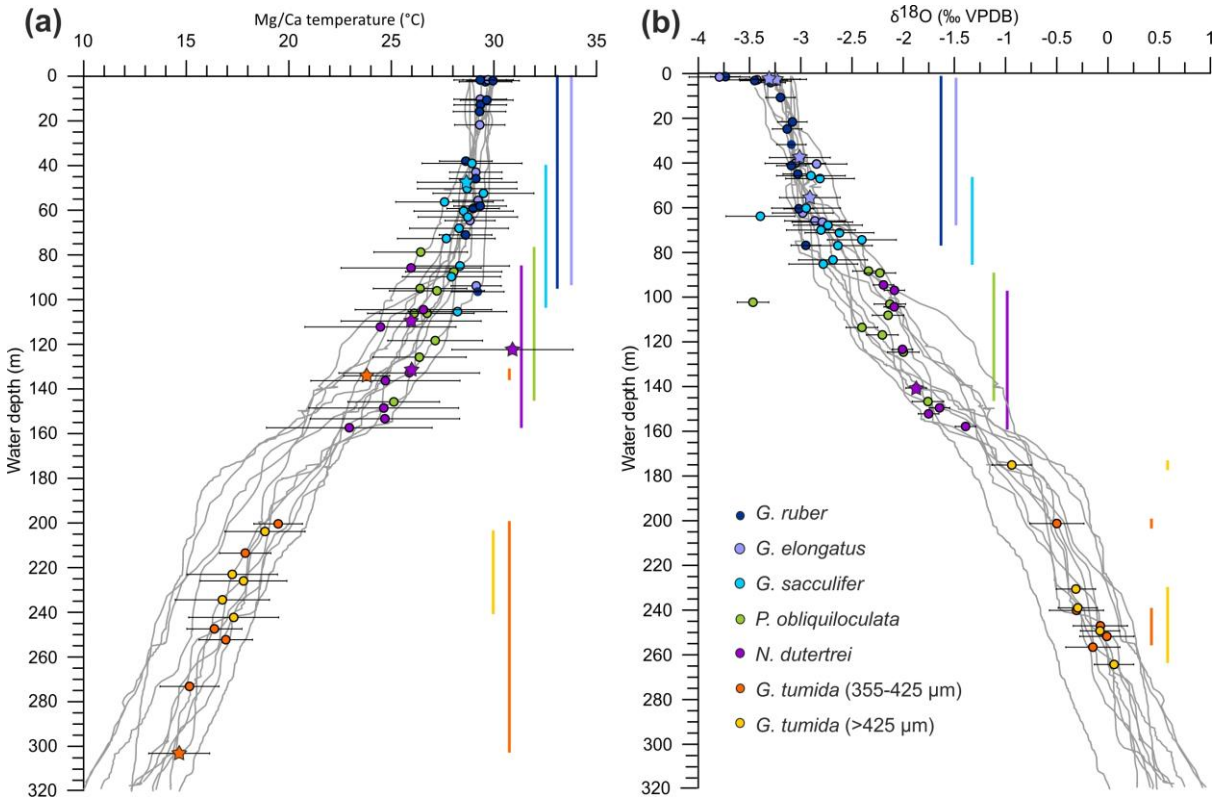

Figure 7. (a) Mg/Ca temperatures calculated by applying the newly established species-specific calibrations projected on CTD temperature profiles (grey lines). Horizontal bars denote temperature errors, calculated following the method described in *Mohtadi et al.* [2014]. Colored vertical bars indicate calcification depth ranges resulting from the application of our species-specific Mg/Ca-temperature calibrations. (b) For comparison, we show shell $\delta^{18}O$-derived calcification depth estimates for all species in combination. Gray lines indicate depth profiles of predicted $\delta^{18}Oc$ calculated from CTD casts. Samples where only Mg/Ca or $\delta^{18}O$ measurements are available are marked with stars.

6. Conclusions

We presented novel, paired Mg/Ca and $\delta^{18}O$ measurements on multispecies planktic foraminifera tests from accurately dated modern surface sediments in combination with water column data (CTD and $\delta^{18}O_{SW}$) from the WPWP. Based on CTD salinity and $\delta^{18}O_{SW}$ we establish new $\delta^{18}O_{SW}$-salinity regressions for surface (mixed layer) and subsurface (thermocline) waters (NPTW and SPTW) in the WPWP. Our data imply that it is reasonable to apply different $\delta^{18}O_{SW}$-salinity regressions for surface and thermocline water masses. Due

763 to very similar regression lines for the Philippines and PNG areas, individual regressions for
764 sub(surface) waters from both areas can be combined into more robust equations representing
765 the entire study area. These equations are $\delta^{18}O_{SW}$ = 0.37*S-12.4 for surface and $\delta^{18}O_{SW}$ =
766 0.33*S-11.0 for thermocline waters.
767
768 Shell $\delta^{18}O$-derived estimates reveal that the calcification depths of planktic foraminifera
769 offshore the Philippines and offshore PNG are very similar. Our estimates match results from
770 other areas, and reveal that, also in the WPWP, *G. ruber* and *G. elongatus* reflect mixed layer
771 conditions (0-80 m), *G. sacculifer* reflects bottom of mixed layer and uppermost thermocline
772 conditions (45-85 m). *P. obliquiloculata* and *N. dutertrei* preserve upper (90-160 m) and *G.*
773 *tumida* lower thermocline conditions (230-265 m). Hence, our data imply that these species are
774 the best choice to reconstruct thermocline conditions in the WPWP. *N. dutertrei* inhabits a
775 slightly larger depth range than *P. obliquiloculata* in the WPWP. Therefore, *P. obliquiloculata*
776 might be more suitable to reconstruct the upper thermocline. Previous thermocline
777 reconstructions that are based on other species need to be reconsidered in face of the new
778 results. For example, shell $\delta^{18}O$ does not indicate different habitat depths for *G. ruber* and *G.*
779 *elongatus*. Hence, for the WPWP, the data do not support the use of *G. ruber – G. elongatus*
780 records to reconstruct variations in the vertical structure of the upper water column.
781
782 Our newly established regional multispecies Mg/Ca-temperature regression is within the range
783 of published multispecies and species-specific Mg/Ca-temperature calibrations (Mg/Ca = 0.26
784 exp 0.097*T as calculated using reduced major axis regression). However, the Mg/Ca
785 temperature relation of most individual species is more accurately described by species-specific
786 calibrations. We find that the regional regressions for *G. ruber*, *G. elongatus* and *G. tumida* are
787 similar to the species-specific or multispecies equations published by *Dekens et al.* [2002] and
788 *Anand et al.* [2003]. Calcification temperatures of *G. sacculifer*, *P. obliquiloculata* and *N.*
789 *dutertrei* are exceptionally warm in the western tropical Pacific and thus, require regional,
790 species-specific calibrations. The application of previously published calibrations would
791 underestimate the calcification temperatures of these species. Using a reduced major axis
792 regression we calculate the species-specific calibration Mg/Ca = 0.24 exp 0.097*T for *G.*
793 *sacculifer* and Mg/Ca = 0.21 exp 0.097*T for *P. obliquiloculata* and *N. dutertrei*. Nevertheless,
794 further studies are needed to confirm the applicability of these calibrations for the open Pacific
795 Ocean and for paleo-reconstructions.

Acknowledgments

We would like to thank the captains, crews, and the scientific shipboard parties of expeditions SO–228 and RR–1313. We thank Henning Kuhnert, Birgit Meyer-Schack and Ryan Bu for technical assistance. John Southon (UC Irvine) is acknowledged for performing radiocarbon measurements. GeoB sample material was stored, curated and supplied by the GeoB Core Repository at the MARUM – Center for Marine Environmental Sciences, University of Bremen, Germany. RR samples were provided by the Rutgers Core Repository. We thank two anonymous reviewers for their constructive comments, which helped to improve the quality of our manuscript. The work is funded by the DFG-Research Center / Cluster of Excellence "The Ocean in the Earth System", the BMBF project 03G0228A (EISPAC) and by the NSF project OCE1131371. The data reported in this paper will be made available on Pangaea (www.pangaea.de) and WDS (www.icsu-wds.org).

References

Allen, K. A., B. Hönisch, S. M. Eggins, L. L. Haynes, Y. Rosenthal, and J. Yu (2016), Trace element proxies for surface ocean conditions: A synthesis of culture calibrations with planktic foraminifera, *Geochimica et Cosmochimica Acta*, *193*, 197-221, doi:10.1016/j.gca.2016.08.015.

Anand, P., H. Elderfield, and M. H. Conte (2003), Calibration of Mg/Ca thermometry in planktonic foraminifera from a sediment trap time series, *Paleoceanography*, *18*(2), 1050, doi:10.1029/2002PA000846.

Andreasen, D. J., and A. C. Ravelo (1997), Tropical Pacific Ocean thermocline depth reconstructions for the Last Glacial Maximum, *Paleoceanography*, *12*(3), 395-413, doi:10.1029/97PA00822.

Arbuszewski, J., P. deMenocal, A. Kaplan, and E. C. Farmer (2010), On the fidelity of shell-derived $\delta^{18}O_{seawater}$ estimates, *Earth and Planetary Science Letters*, *300*(3-4), 185-196, doi:10.1016/j.epsl.2010.10.035.

Aurahs, R., Y. Treis, K. Darling, and M. Kucera (2011), A revised taxonomic and phylogenetic concept for the planktonic foraminifer species Globigerinoides ruber based on molecular and morphometric evidence, *Marine Micropaleontology*, *79*(1-2), 1-14, doi:10.1016/j.marmicro.2010.12.001.

Barker, S., M. Greaves, and H. Elderfield (2003), A study of cleaning procedures used for foraminiferal Mg/Ca paleothermometry, *Geochem Geophy Geosy*, *4*(9), 8407, doi:10.1029/2003GC000559.

Beaufort, L., T. de Garidel-Thoron, A. C. Mix, and N. G. Pisias (2001), ENSO-like forcing on oceanic primary production during the Late Pleistocene, *Science*, *293*(5539), 2440-2444, doi:10.1126/science.293.5539.2440.

Bemis, B. E., H. J. Spero, J. Bijma, and D. W. Lea (1998), Reevaluation of the oxygen isotopic composition of planktonic foraminifera: Experimental results and revised paleotemperature equations, *Paleoceanography*, *13*(2), 150-160, doi:10.1029/98pa00070.

Berger, W. H., M. C. Bonneau, and F. L. Parker (1982), Foraminifera on the deep-sea floor: lysocline and dissolution rate, *Oceanologica Acta*, *5*, 249-258.

Böhm, F., M. M. Joachimski, H. Lehnert, G. Morgenroth, W. Kretschmer, J. Vacelet, and W.-C. Dullo (1996), Carbon isotope records from extant Caribbean and South Pacific sponges: Evolution of $\delta^{13}C$ in surface water DIC, *Earth and Planetary Science Letters*, *139*(1), 291-303, doi:10.1016/0012-821X(96)00006-4.

Bolliet, T., A. Holbourn, W. Kuhnt, C. Laj, C. Kissel, L. Beaufort, M. Kienast, N. Andersen, and D. Garbe-Schonberg (2011), Mindanao Dome variability over the last 160 kyr: Episodic glacial cooling of the West Pacific Warm Pool, *Paleoceanography*, *26*(1), PA1208, doi:10.1029/2010pa001966.

Bouvier-Soumagnac, Y., and J. C. Duplessy (1985), Carbon and oxygen isotopic composition of planktonic foraminifera from laboratory culture, plankton tows and Recent sediment: implications for the reconstruction of paleoclimatic conditions and of the global carbon cycle, *Journal of Foraminiferal Research*, *15*, 302-320.

Boyle, E. A., and L. D. Keigwin (1985), Comparison of Atlantic and Pacific paleochemical records for the last 215,000 years: changes in deep ocean circulation and chemical inventories, *Earth and Planetary Science Letters*, *76*, 135-150.

Cléroux, C., E. Cortijo, P. Anand, L. Labeyrie, F. Bassinot, N. Caillon, and J.-C. Duplessy (2008), Mg/Ca and Sr/Ca ratios in planktonic foraminifera: Proxies for upper water column temperature reconstruction, *Paleoceanography*, *23*(3), PA3214, doi:10.1029/2007pa001505.

Craig, H., and L. I. Gordon (1965), Deuterium and oxygen-18 variations in the ocean and the marine atmosphere, in *Stable isotope in oceanographic studies and paleotemperatures*, edited by E. Tongiorgi, pp. 9-130, Spoleto, Pisa (Consiglio Nazionale delle Ricerche, Laboratorio di Geologia Nucleare).

de Garidel-Thoron, T., Y. Rosenthal, L. Beaufort, E. Bard, C. Sonzogni, and A. C. Mix (2007), A multiproxy assessment of the western equatorial Pacific hydrography during the last 30 kyr, *Paleoceanography*, *22*, PA3204, doi:3210.1029/2006PA001269.

Dekens, P. S., D. W. Lea, D. K. Pak, and H. J. Spero (2002), Core top calibration of Mg/Ca in tropical foraminifera: Refining paleotemperature estimation, *Geochemistry, Geophysics, Geosystems*, *3*(4), 1022, doi:10.1029/2001GC000200.

DiNezio, P. N., A. Clement, G. A. Vecchi, B. Soden, A. J. Broccoli, B. L. Otto-Bliesner, and P. Braconnot (2011), The response of the Walker circulation to Last Glacial Maximum forcing: Implications for detection in proxies, *Paleoceanography*, *26*(3), PA3217, doi:10.1029/2010PA002083.

Elderfield, H., and G. Ganssen (2000), Past temperature and $\delta^{18}O$ of surface ocean waters inferred from foraminiferal Mg/Ca ratios, *Nature*, *405*(6785), 442-445, doi:10.1038/35013033.

Epstein, S., and T. Mayeda (1953), Variation of O^{18} content of waters from natural sources, *Geochimica et Cosmochimica Acta*, *4*, 213-224.

Evans, D., B. S. Wade, M. Henehan, J. Erez, and W. Müller (2016), Revisiting carbonate chemistry controls on planktic foraminifera Mg / Ca: implications for sea surface temperature and hydrology shifts over the Paleocene–Eocene Thermal Maximum and Eocene–Oligocene transition, *Climate of the Past*, *12*(4), 819-835, doi:10.5194/cp-12-819-2016.

Fairbanks, R. G. (1982), The origin of Continental Shelf and Slope Water in the New York Bight of Maine: Evidence from $H_2{}^{18}O/H_2{}^{16}O$ Ratio Measurements, *Journal of Geophysical Research*, *87*(C8), 5796-5808.

Fairbanks, R. G., C. D. Charles, and J. D. Wright (1992), Origin of global meltwater pulses, in *Radiocarbon after four decades*, edited by R. E. Taylor, pp. 473-500, Springer Verlag.

Fairbanks, R. G., M. N. Evans, J. L. Rubenstone, R. A. Mortlock, K. Broad, M. D. Moore, and C. D. Charles (1997), Evaluating climate indices and their geochemical proxies measured in corals, *Coral Reefs*, *16*, 93-100.

Farmer, E. C., A. Kaplan, P. B. de Menocal, and J. Lynch-Stieglitz (2007), Corroborating ecological depth preferences of planktonic foraminifera in the tropical Atlantic with the stable oxygen isotope ratios of core top specimens, *Paleoceanography*, *22*(3), doi:10.1029/2006PA001361.

Ferguson, J. E., G. M. Henderson, M. Kucera, and R. E. M. Rickaby (2008), Systematic change of foraminiferal Mg/Ca ratios across a strong salinity gradient, *Earth and Planetary Science Letters*, *265*(1-2), 153-166, doi:10.1016/j.epsl.2007.10.011.

Fine, R. A., R. Lukas, F. M. Bingham, M. J. Warner, and R. H. Gammon (1994), The western equatorial Pacific - a water mass crossroads, *Journal of Geophysical Research*, *99*(C12), 25063-25080, doi:10.1029/94jc02277.

Friedli, H., H. Lötscher, H. Oeschger, U. Siegenthaler, and B. Stauffer (1986), Ice core record of the $^{13}C/^{12}C$ ratio of atmospheric CO_2 in the past two centuries, *Nature*, *324*, 237-238.

Gagan, M. K., E. J. Hendy, S. G. Haberle, and W. S. Hantoro (2004), Post-glacial evolution of the Indo-Pacific Warm Pool and El Niño-Southern oscillation, *Quaternary International*, *118-119*, 127-143, doi:10.1016/s1040-6182(03)00134-4.

Gordon, A. L. (1986), Interocean exchange of thermocline water, *Journal of Geophysical Research*, *91*(C4), 5037, doi:10.1029/JC091iC04p05037.

Hertzberg, J. E., and M. W. Schmidt (2013), Refining *Globigerinoides ruber* Mg/Ca paleothermometry in the Atlantic Ocean, *Earth and Planetary Science Letters*, *383*, 123-133, doi:10.1016/j.epsl.2013.09.044.

Higgins, H. W., D. J. Mackey, and L. Clementson (2006), Phytoplankton distribution in the Bismarck Sea north of Papua New Guinea: The effect of the Sepik River outflow, *Deep-Sea Research Part I: Oceanographic Research Papers*, *53*(11), 1845-1863, doi:10.1016/j.dsr.2006.09.001.

Hönisch, B., K. A. Allen, D. W. Lea, H. J. Spero, S. M. Eggins, J. Arbuszewski, P. deMenocal, Y. Rosenthal, A. D. Russell, and H. Elderfield (2013), The influence of salinity on Mg/Ca in planktic foraminifers – Evidence from cultures, core-top sediments and complementary $\delta^{18}O$, *Geochimica et Cosmochimica Acta*, *121*, 196-213, doi:10.1016/j.gca.2013.07.028.

Hut, G. (1987), Consultants group meeting on stable isotopic reference samples for geochemical and hydrological investigations, edited, p. 42, International Atomic Energy Agency, Vienna.

Isobe, T., E. D. Feigelson, M. G. Akritas, and G. J. Babu (1990), Linear Regression in Astronomy I., *The Astrophysical Journal*, *364*, 104-113.

Kawahata, H. (2005), Stable isotopic composition of two morphotypes of Globigerinoides ruber (white) in the subtropical gyre in the North Pacific, *Paleontological Research*, *9*(1), 27-35.
Kawahata, H., A. Nishimura, and M. K. Gagan (2002), Seasonal change in foraminiferal production in the western equatorial Pacific warm pool: evidence from sediment trap experiments, *Deep-Sea Research Part II: Topical Studies in Oceanography*, *49*(13-14), 2783-2800, doi:10.1016/S0967-0645(02)00058-9.
Kim, S.-T., and J. R. O'Neil (1997), Equilibrium and nonequilibrium oxygen isotope effects in synthetic carbonates, *Geochim Cosmochim Ac*, *61*(16), 3461-3475, 10.1016/s0016-7037(97)00169-5.
Kısakürek, B., A. Eisenhauer, F. Böhm, D. Garbe-Schönberg, and J. Erez (2008), Controls on shell Mg/Ca and Sr/Ca in cultured planktonic foraminiferan, *Globigerinoides ruber* (white), *Earth and Planetary Science Letters*, *273*(3-4), 260-269, doi:10.1016/j.epsl.2008.06.026.
Kuroyanagi, A., and H. Kawahata (2004), Vertical distribution of living planktonic foraminifera in the seas around Japan, *Marine Micropaleontology*, *53*(1-2), 173-196, DOI 10.1016/j.marmicro.2004.06.001.
Lea, D. W., T. A. Mashiotta, and H. J. Spero (1999), Controls on magnesium and strontium uptake in planktonic foraminifera determined by live culturing, *Geochimica Et Cosmochimica Acta*, *63*(16), 2369-2379, doi:10.1016/S0016-7037(99)00197-0.
Lea, D. W., D. K. Pak, and H. J. Spero (2000), Climate impact of late quaternary equatorial pacific sea surface temperature variations, *Science*, *289*(5485), 1719-1724.
Leech, P. J., J. Lynch-Stieglitz, and R. Zhang (2013), Western Pacific thermocline structure and the Pacific marine Intertropical Convergence Zone during the Last Glacial Maximum, *Earth and Planetary Science Letters*, *363*, 133-143, doi:10.1016/j.epsl.2012.12.026.
LeGrande, A. N., and G. A. Schmidt (2006), Global gridded data set of the oxygen isotopic composition in seawater, *Geophysical Research Letters*, *33*(12), doi:10.1029/2006gl026011.
LeGrande, A. N., and G. A. Schmidt (2011), Water isotopologues as a quantitative paleosalinity proxy, *Paleoceanography*, *26*(3), doi:10.1029/2010pa002043.
Locarnini, R. A., et al. (2013), *World Ocean Atlas 2013, Volume 1: Temperature.*, U.S. Government Printing Office, Washington, D.C.
Lončarić, N., F. J. C. Peeters, D. Kroon, and G.-J. A. Brummer (2006), Oxygen isotope ecology of recent planktic foraminifera at the central Walvis Ridge (SE Atlantic), *Paleoceanography*, *21*(3), doi:10.1029/2005pa001207.
Martin, P. A., and D. W. Lea (2002), A simple evaluation of cleaning procedures on fossil benthic foraminiferal Mg/Ca, *Geochem Geophy Geosy*, *3*(10), 1-8, doi:10.1029/2001gc000280.
Mathien-Blard, E., and F. Bassinot (2009), Salinity bias on the foraminifera Mg/Ca thermometry: Correction procedure and implications for past ocean hydrographic reconstructions, *Geochemistry, Geophysics, Geosystems*, *10*(12), doi:10.1029/2008gc002353.
McConnell, M. C., and R. C. Thunell (2005), Calibration of the planktonic foraminiferal Mg/Ca paleothermometer: Sediment trap results from the Guaymas Basin, Gulf of California, *Paleoceanography*, *20*(2), doi:10.1029/2004pa001077.
Mohtadi, M., S. Steinke, J. Groeneveld, H. G. Fink, T. Rixen, D. Hebbeln, B. Donner, and B. Herunadi (2009), Low-latitude control on seasonal and interannual changes in planktonic foraminiferal flux and shell geochemistry off south Java: A sediment trap study, *Paleoceanography*, *24*(1), PA1201, doi:10.1029/2008pa001636.
Mohtadi, M., D. W. Oppo, A. Luckge, R. DePol-Holz, S. Steinke, J. Groeneveld, N. Hemme, and D. Hebbeln (2011), Reconstructing the thermal structure of the upper ocean: Insights from planktic foraminifera shell chemistry and alkenones in modern sediments of the tropical eastern Indian Ocean, *Paleoceanography*, *26*(3), PA3219, doi:10.1029/2011pa002132.
Mohtadi, M., M. Prange, D. W. Oppo, R. De Pol-Holz, U. Merkel, X. Zhang, S. Steinke, and A. Luckge (2014), North Atlantic forcing of tropical Indian Ocean climate, *Nature*, *509*(7498), 76-80, doi:10.1038/nature13196.
Mohtadi, M., et al. (2013), Report and preliminary results of RV SONNE cruise SO-228, Kaohsiung-Townsville, 04.05.2013- 23.06.2013, EISPAC-WESTWIND-SIODP. Berichte aus dem MARUM und dem Fachbereich Geowissenschaften der Universität Bremen, 295, 110 pp. urn:nbn:de:gbv:46-00103343-13.
Morimoto, M. (2002), Salinity records for the 1997–98 El Niño from Western Pacific corals, *Geophysical Research Letters*, *29*(11), doi:10.1029/2001gl013521.
Mulitza, S., D. Boltovskoy, B. Donner, H. Meggers, A. Paul, and G. Wefer (2003), Temperature:$\delta^{18}O$ relationships of planktonic foraminifera collected from surface waters, *Palaeogeography, Palaeoclimatology, Palaeoecology*, *202*(1-2), 143-152, doi:10.1016/s0031-0182(03)00633-3.
Niebler, H.-S., H.-W. Hubberten, and G. Gersonde (1999), Oxygen isotope values of planktic foraminifera: a tool for the reconstruction of surface water stratification, in *Use of Proxies in Paleoceanography: Examples from the South Atlantic*, edited by G. Fischer and G. Wefer, pp. 165-189, Springer-Verlag, Berlin, Heidelberg.
Nürnberg, D., J. Bijma, and C. Hemleben (1996), Assessing the reliability of magnesium in foraminiferal calcite as a proxy for water mass temperatures, *Geochimica et Cosmochimica Acta*, *60*(5), 803-814.

Nürnberg, D., A. Müller, and R. R. Schneider (2000), Paleo-sea surface temperature calculations in the equatorial east Atlantic from Mg/Ca ratios in planktic foraminifera: A comparison to sea surface temperature estimates from Uk37, oxygen isotopes, and foraminiferal transfer function, *Paleoceanography*, *15*(1), 124-134, 10.1029/1999PA000370.

Patrick, A., and R. C. Thunell (1997), Tropical Pacific sea surface temperatures and upper water column thermal structure during the Last Glacial Maximum, *Paleoceanography*, *12*(5), 649-657, doi:10.1029/97pa01553.

Peeters, F. J. C., G.-J. A. Brummer, and G. Ganssen (2002), The effect of upwelling on the distribution and stable isotope composition of *Globigerina bulloides* and *Globigerinoides ruber* (planktic foraminifera) in modern surface waters of the NW Arabian Sea, *Global and Planetary Change*, *34*(3-4), 269-291, doi:10.1016/S0921-8181(02)00120-0.

Radenac, M.-H., and M. Rodier (1996), Nitrate and chlorophyll distributions in relation to thermohaline and current structures in the western tropical Pacific during 1985-1989, *Deep Sea Research Part II: Topical Studies in Oceanography*, *4-6*, 725-752.

Radenac, M. H., F. Leger, M. Messie, P. Dutrieux, C. Menkes, and G. Eldin (2016), Wind-driven changes of surface current, temperature, and chlorophyll observed by satellites north of New Guinea, *J Geophys Res-Oceans*, *121*(4), 2231-2252, 10.1002/2015JC011438.

Ravelo, A. C., and C. Hillaire-Marcel (2007), Chapter Eighteen The Use of Oxygen and Carbon Isotopes of Foraminifera in Paleoceanography, *1*, 735-764, doi:10.1016/s1572-5480(07)01023-8.

Regenberg, M., S. Steph, D. Nürnberg, R. Tiedemann, and D. Garbe-Schönberg (2009), Calibrating Mg/Ca ratios of multiple planktonic foraminiferal species with δ^{18}O-calcification temperatures: Paleothermometry for the upper water column, *Earth and Planetary Science Letters*, *278*(3-4), 324-336, doi:10.1016/j.epsl.2008.12.019.

Regoli, F., T. de Garidel-Thoron, K. Tachikawa, Z. Jian, L. Ye, A. W. Droxler, G. Lenoir, M. Crucifix, N. Barbarin, and L. Beaufort (2015), Progressive shoaling of the equatorial Pacific thermocline over the last eight glacial periods, *Paleoceanography*, *30*(5), 439-455, doi:10.1002/2014pa002696.

Rickaby, R. E. M., and P. Halloran (2005), Cool La Niña During the Warmth of the Pliocene?, *Science*, *307*(5717), 1948-1952, doi:10.1126/science.1104666.

Rippert, N., D. Nürnberg, J. Raddatz, E. Maier, E. Hathorne, J. Bijma, and R. Tiedemann (2016), Constraining foraminiferal calcification depths in the western Pacific warm pool, *Marine Micropaleontology*, *128*, 14-27, doi:10.1016/j.marmicro.2016.08.004.

Rosenthal, Y., and G. P. Lohmann (2002), Accurate estimation of sea surface temperatures using dissolution-corrected calibrations for Mg/Ca paleothermometry, *Paleoceanography*, *17*(3), 16-11-16-16, 1044, 10.1029/2001pa000749.

Rosenthal, Y., E. A. Boyle, and N. Slowey (1997), Temperature control on the incorporation of magnesium, strontium, fluorine, and cadmium into benthic foraminiferal shells from Little Bahama Bank: Prospects for thermocline paleoceanography, *Geochimica Et Cosmochimica Acta*, *61*(17), 3633-3643, doi:10.1016/S0016-7037(97)00181-6.

Rosenthal, Y., M. P. Field, and R. M. Sherrell (1999), Precise determination of element/calcium ratios in calcareous samples using sector field inductively coupled plasma mass spectrometry, *Analytical Chemistry*, *71*(15), 3248-3253, doi:10.1021/AC981410x.

Rosenthal, Y., et al. (2004), Interlaboratory comparison study of Mg/Ca and Sr/Ca measurements in planktonic foraminifera for paleoceanographic research, *Geochem Geophy Geosy*, *5*, doi:10.1029/2003GC000650.

Russell, A. D., B. Hönisch, H. J. Spero, and D. W. Lea (2004), Effects of seawater carbonate ion concentration and temperature on shell U, Mg, and Sr in cultured planktonic foraminifera, *Geochimica et Cosmochimica Acta*, *68*(21), 4347-4361, 10.1016/j.gca.2004.03.013.

Sagawa, T., Y. Yokoyama, M. Ikehara, and M. Kuwae (2012), Shoaling of the western equatorial Pacific thermocline during the last glacial maximum inferred from multispecies temperature reconstruction of planktonic foraminifera, *Palaeogeography, Palaeoclimatology, Palaeoecology*, *346–347*, 120-129, doi:10.1016/j.palaeo.2012.06.002.

Schlitzer, R. (2014), Ocean Data View, odv.awi.de, edited.

Shackleton, N. (1974), Attainment of isotopic equilibrium between ocean water and the benthonic foraminifera genus *Uvigerina*: Isotopic changes in the ocean during the last glacial, in *Les méthodes quantitatives d'étude des variations du climat au cours du Pléistocène*, edited by L. Labeyrie, pp. 203-209, CNRS, Paris.

Spero, H. J., K. M. Mielke, E. M. Kalve, D. W. Lea, and D. K. Pak (2003), Multispecies approach to reconstructing eastern equatorial Pacific thermocline hydrography during the past 360 kyr, *Paleoceanography*, *18*(1), doi:10.1029/2002PA000814.

Spero, H. J., S. M. Eggins, A. D. Russell, L. Vetter, M. R. Kilburn, and B. Hönisch (2015), Timing and mechanism for intratest Mg/Ca variability in a living planktic foraminifer, *Earth and Planetary Science Letters*, *409*, 32-42, 10.1016/j.epsl.2014.10.030.

Steinke, S., H.-Y. Chiu, P.-S. Yu, C.-C. Shen, L. Löwemark, H.-S. Mii, and M.-T. Chen (2005), Mg/Ca ratios of two *Globigerinoides ruber* (white) morphotypes: Implications for reconstructing past tropical/subtropical surface water conditions, *Geochemistry, Geophysics, Geosystems*, *6*(11), doi:10.1029/2005gc000926.

Steph, S., M. Regenberg, R. Tiedemann, S. Mulitza, and D. Nürnberg (2009), Stable isotopes of planktonic foraminifera from tropical Atlantic/Caribbean core-tops: Implications for reconstructing upper ocean stratification, *Marine Micropaleontology*, *71*(1-2), 1-19, doi:10.1016/j.marmicro.2008.12.004.

Tachikawa, K., A. Timmermann, L. Vidal, C. Sonzogni, and O. E. Timm (2014), CO_2 radiative forcing and Intertropical Convergence Zone influences on western Pacific warm pool climate over the past 400 ka, *Quaternary Science Reviews*, *86*(0), 24-34, doi:10.1016/j.quascirev.2013.12.018.

Thirumalai, K., J. N. Richey, T. M. Quinn, and R. Z. Poore (2014), Globigerinoides ruber morphotypes in the Gulf of Mexico: a test of null hypothesis, *Scientific reports*, *4*, 6018, doi:10.1038/srep06018.

Thunell, R., E. Tappa, C. Pride, and E. Kincaid (1999), Sea-surface temperature anomalies associated with the 1997/1998 El Niño recorded in the oxygen isotope composition of planktonic foraminifera, *Geology*, *27*(9), 843-846.

Tsuchiya, M., R. Lukas, and R. Fine (1989), Source Waters of the Pacific Equatorial Undercurrent, *Progress in Oceanography*, *23*, 46.

van Geldern, R., and J. A. C. Barth (2012), Optimization of instrument setup and post-run corrections for oxygen and hydrogen stable isotope measurements of water by isotope ratio infrared spectroscopy (IRIS), *Limnology and Oceanography: Methods*, *10*(12), 1024-1036, doi:10.4319/lom.2012.10.1024.

Vecchi, G. A., B. J. Soden, A. T. Wittenberg, I. M. Held, A. Leetmaa, and M. J. Harrison (2006), Weakening of tropical Pacific atmospheric circulation due to anthropogenic forcing, *Nature*, *441*(7089), 73-76, doi:10.1038/nature04744.

Wang, L. J. (2000), Isotopic signals in two morphotypes of *Globigerinoides ruber* (white) from the South China Sea: implications for monsoon climate change during the last glacial cycle, *Palaeogeogr Palaeocl*, *161*(3-4), 381-394, doi:10.1016/S0031-0182(00)00094-8.

Watkins, J. M., A. C. Mix, and J. Wilson (1996), Living planktic foraminifera: Tracers of circulation and productivity regimes in the central equatorial Pacific, *Deep Sea Research Part II: Topical Studies in Oceanography*, *43*(4-6), 26.

Xu, J. A., W. Kuhnt, A. Holbourn, M. Regenberg, and N. Andersen (2010), Indo-Pacific Warm Pool variability during the Holocene and Last Glacial Maximum, *Paleoceanography*, *25*(4), PA4230, doi:10.1029/2010PA001934.

Yamasaki, M., A. Sasaki, M. Oda, and H. Domitsu (2008), Western equatorial Pacific planktic foraminiferal fluxes and assemblages during a La Niña year (1999), *Marine Micropaleontology*, *66*(3-4), 304-319, doi:10.1016/j.marmicro.2007.10.006.

Zenk, W., G. Siedler, A. Ishida, J. Holfort, Y. Kashino, Y. Kuroda, T. Miyama, and T. J. Müller (2005), Pathways and variability of the Antarctic Intermediate Water in the western equatorial Pacific Ocean, *Progress in Oceanography*, *67*, 245-281, doi:10.1016/j.pocean.2005.05.003.

Zweng, M. M., et al. (2013), *World Ocean Atlas 2013, Volume 2: Salinity*, Washington, D.C.